AUTHOR	Tehrani Mojan Maleki, Akhtari Mohammadreza, Kasaeian Alibakhsh, Rad Mohammad Amin Vaziri, Toopshekan Ashkan, Motlagh Maryam Sadeghi
TITLE	Techno-economic investigation of a hybrid biomass renewable energy system to achieve the goals of SDG-17 in deprived areas of Iran
YEAR	2023
DOI	http://dx.doi.org/10.1016%2Fj.enconman.2023.117319
VERSION	Author's accepted manuscript
COPYRIGHT	License: CC BY NC ND
CITATION	Mojan Maleki Tehrani, Mohammadreza Akhtari, Alibakhsh Kasaeian, Mohammad Amin Vaziri Rad, Ashkan Toopshekan, Maryam Sadeghi Motlagh, Techno-economic investigation of a hybrid biomass renewable energy system to achieve the goals of SDG-17 in deprived areas of Iran, Energy Conversion and Management, Volume 291, 2023, 117319, ISSN 0196-8904, https://doi.org/10.1016/j.enconman.2023.117319.

Techno-economic Investigation of a Hybrid Biomass Renewable Energy System to Achieve the Goals of SDG-17 in Deprived Areas of Iran

Mojan Maleki Tehrani[1], Mohammadreza Akhtari[2, *], Alibakhsh Kasaeian[3, *], Mohammad Amin Vaziri Rad[3], Ashkan Toopshekan[3], Maryam Sadeghi Motlagh[3]

[1] Faculty of Electrical & Computer Engineering, I. Azad University TNB, Tehran, Iran.
[2] Industrial Engineering and Management, Department of Mechanical and Materials Engineering, University of Turku, Turun Yliopisto, 20014 Turku, Finland.
[3] Faculty of New Sciences and Technologies, University of Tehran, Tehran, Iran.

*Corresponding author: Alibakhsh Kasaeian; akasa@ut.ac.ir

Abstract

Improving the quality of life in deprived areas is one of the main programs of the United Nations, highlighting the significance of a clean and reliable power supply for sustainable development. This study focuses on the configuration of hybrid renewable energy systems (HRES) in Iran's northern and southern rural areas, utilizing a combination of wind turbines, storage banks, photovoltaic panels, biogas, and diesel generators. These regions possess animal- and agriculture-based biomass resources that can effectively meet their primary residential energy needs. This study highlights the importance of employing multi-criteria decision-making (MCDM) for selecting suitable hybrid renewable energy systems (HRES) in rural areas. By incorporating a novel objective weighting process based on the SDG-17 framework, the study considers a range of criteria, including economic, environmental, energy security, and technical factors. Furthermore, the validation of HOMER's accuracy in sizing renewable energy systems with particle swarm optimization (PSO) has demonstrated the significant capability of the primary model. The results demonstrate that relying solely on economically optimal scenarios may not align with CO2 emissions, energy efficiency, and reliability goals. Utilizing the HOMER-MCDM method, the study achieves a more optimal combination of energy systems, considering multiple aspects of sustainable development beyond economic efficiency. For the climates of northern and southern rural regions of Iran, the study identifies the PV/WT/Bio/battery system as the best solution, with levelized costs of electricity (COE) of 0.251 and 0.219 $/kWh, respectively. This configuration relies entirely on local resources, emits nearly zero emissions, and provides power to the communities. Additionally, a sensitivity analysis assesses the impact of changes in capital costs of power generation components and the potential of renewable resources. Adjusting the investment costs of PV and WT systems between 0.7 and 1.3 times their original values results in a COE range of 0.198 to 0.233 $/kWh, representing a decrease of 9.2% and an increase of 6.9% compared to the initial operation, respectively.

Keywords: Biomass; Renewable energy; Sustainable development; Multi-criteria decision making; Optimization.

Nomenclature

BG	Biogas Generator	**Q**	The total energy in the beginning (kWh)
CRF	Capital Recovery Factor	**R**	Gas constant (J⁄kgK)
C_{ann}	Annualized cost	**R**	Lifetime of the project (yr)
C_{tot}	Total cost in the project lifetime ($)	R_{comp}	The lifetime of the components (year)
C_{rep}	Replacement cost	**S**	Salvage ($)
DG	Diesel Generator	**T**	Temperature (˚C)
E_{served}	Total electrical load served (kWh/year)	T_{α}	Temperature of ambient (˚C)
f	Inflation rate (%)	T_c	Temperature of PV cell (˚C)
f_{gas}	Gasification ratio (kg, gas/kg, biomass)	Y_{PV}	PV rated power (kW)
f_{PV}	Derating factor of PV (%)	Z_0	Length of surface roughness (m)
g	Gravitational acceleration (m/s^2)	Z_{snem}	The height of the anemometer (m)
G_T	Solar radiation hitting PV (kW⁄m^2)	Z_{hub}	Height of the wind turbine’s height (m)
i	Annual discount rate	**SDG**	Sustainable Development Goals
KBM	Kinetic battery model	U_{anem}	Wind speed at anemometer height (m/s)
LHV	The lower heating value	U_{hub}	Wind speed at hub height (m/s)
LHV_{bg}	Lower heating values of biogas		***Greek Symbols***
N_{batt}	Number of batteries	λ_P	Temperature coefficient of power
NPC	Net present cost ($)	α	Solar absorptance of PV
OC	Operating cost	α_c	Maximum charge rate of storage (A/Ah)
P	Pressure (Pa)	α_p	Temperature coefficient of power (%/(˚C))
P_{CH_4}	Available methane in the biogas (%)	Δt	Temperature difference
P_e	Biogas generator power output (kW)	τ	Solar transmittance of PV
PV	Photovoltaic panel	η	Efficiency (%)
Q_{bg}	The biogas flow rate (m^3/h)	ρ	Real air density (kg/m^3)

1. Introduction

The energy sector has a profound impact on several crucial factors of national development, such as economic growth, advancements in healthcare, and the facilitation of remote working, among others. This underscores the undeniable significance and the increasing demand for a diverse range of energy sources [1]. It is estimated that more than one billion people live proper access to electricity [2], of which only 20% reside in cities [3]. The world's renewable electricity generation is projected to increase from 25% in 2018 to 65% in 2030, aiming for 90% of total power generation in 2050, based on the 1.5 °C global warming scenario [4]. It is projected that 40% of electricity will be generated by renewable energy sources (RE) by 2030, surpassing the demand for coal-based energy, which is expected to be less than 20% by 2040 [5]. Although fossil fuel reserves may not be available in long-term future [6], the demand for electricity is expected to increase in the coming years due to infrastructure and grid improvements, urbanization, economic prosperity, and other factors [7]. However, in order to facilitate the better development of deprived and rural areas, it is essential to implement a sustainable development program that includes the provision of affordable and accessible energy as one of its primary foundations.

The Department of Economic and Social Affairs (DESA) of the United Nations (UN) introduced 17 Sustainable Development Goals (SDGs) and 169 targets through its 2030 Agenda for sustainable development in 2015 [8]. Every nation strives to take short, medium, or long-term actions towards SDGs, of which renewable energy could be considered as the driving force and backbone for the following inevitable development [9]. One of the important SDGs is the seventh item, which emphasizes the importance of accessible, reliable, affordable, modern, and sustainable energy for everyone [10]. Developing and increasing the efficiency of reasonably priced renewable energy aligns with SDG 7, which aims to provide accessible electricity and instruments that use renewable and clean energy to all individuals. Furthermore, this effort also contributes to other objectives related to climate change and ecosystem preservation [11] While solar, wind, and bio resources are the most accessible renewable resources, there has been limited focus on hybrid renewable energy systems (HRESs) to meet the objectives of SDG 17, particularly in less developed countries with significant bio-resources potential.

Renewable technologies can be applied to both small-scale and large-scale units. Pirmohamadi et al. [12] applied an integrated solar thermal and photovoltaic system to optimize a small-scale near-zero energy building in Iran. Their results demonstrated that incorporating the solar thermal system into the building increased the thermal efficiency to over 47% and also resulted in potential financial savings of 318 $. On the other hand, Jahangir et al. [13] implemented a biomass-powered off-grid plant to electrify a large-scale urban load in Iran. Their results showed a COE of less than 0.3 $/kWh, highlighting the attractiveness of biogas generators in enhancing the power supply flexibility of highly renewable energy systems. However, it should be noted that the share of bio-based power in Iran is still very low.

It is projected that the use of biomass as an energy resource will increase from 11 EJ in 2020 to 96 EJ in 2050 worldwide [14]. As a result, policymakers, governments, and energy sectors are increasingly interested in generating energy from biomass [15]. Liquid biofuels and biogas were the two fastest-growing sectors in rural energy production from bio-resources. Biogas ranks second, accounting for 14% of the total electricity generation from biomass, after solid biomass [16]. The main biomass resources for standalone energy systems include animal wastes, agricultural residues, and municipal solid wastes [17]. Compared to diesel-fueled generators in off-grid applications, bio-fueled generators have greater potential to reduce emissions, achieve affordable energy costs, and develop sustainable energy systems.

Several studies have investigated HRESs that integrate biomass-powered systems. A wide range of applications, from grid-connected power systems in developed countries to off-grid systems for power supply in deprived areas, has been investigated by applying biomass-based HRES [18]. The feasibility of using a PV/biomass/wind turbine system to power small-scale mining in Europe was the subject of compelling research by Paneri et al. [19]. They stated that although biogas is known as a clean energy resource, high dependency on biogas generators can lead to high CO_2 production from the direct burning of biogas. Therefore, integrating biogas generators with other renewable technologies such as photovoltaic panels (PV) and wind turbines (WT) is more promising to reduce direct GHG emissions from the energy system. Especially in deprived areas with unreliable power grids, the integration of biomass-powered systems in HRES can contribute to local development and social welfare [20]. Yong et al. [21] demonstrated the attractive socio-economic aspect of

HRESs coupled with biomass in the rural region of Sarawak, Malaysia. Their study highlighted the ability of renewable energy-based systems to reduce greenhouse gas emissions and enhance sustainability, ultimately improving the living standards of local communities in the long term. This integration also has the potential to create job opportunities with the number of jobs per MW increasing from approximately 0.5 for PV systems to 3 for hybrid power plants [22].

Singh et al. [23] optimized the PV/WT/biomass system and compared the performance of the artificial bee colony algorithm and the particle swarm optimization (PSO) method with the HOMER software. The results showed that the PSO algorithm had results more similar to those of the HOMER software, although all three methods differed by less than 1 cent/kWh in the final COE in the range of 0.17-0.18 $/kWh. Kharrich et al. [24] investigated an HRES comprising PV, diesel, biomass, and WT in an area of Saudi Arabia with considerable radiation. They used a metaheuristic algorithm called Giza Pyramids Construction to find the optimized system. The study revealed that the optimal energy system consisted of PV and biomass (1000 tons/year), resulting in a COE of 0.208 $/kWh. El-Sattar et al. [25] demonstrated the capability of the Runge-Kutta algorithm to optimize PV/Bio/battery in rural Indian areas and achieved less than 0.10 $/kWh COE. For a 100% renewable PV/WT/bio/battery system, a COE of 0.057 $/kWh was calculated to meet the peak load of 73.6 MW in India using the HOMER software [26]. In another study conducted by Alshammari and Asumadu [27] in a rural area, it was determined that the combination of PV/Biomass/WT and batteries was the most cost-effective system, outperforming other studied options. The COE for this system was calculated to be 0.254 $/kWh. However, the study also revealed that the inclusion of biomass generators in the system could have negative implications for CO_2 emissions when compared to 100% renewable HRESs.

Biomass could be a promising choice for an HRES in both humid and cold climates where solar irradiation is reduced or in regions that do not have significant wind potential, such as most rural areas in Iran. A study conducted in central regions of Iran demonstrated that integrating HRES with biomass can be economically feasible, even when the region is as far as 2.6 km away from the nearest national power grid [28]. Consequently, the development of renewable HRESs can be more economical than developing grid infrastructures for these off-grid regions [29]. The study on the most economically viable bio-resource for power production has been conducted in different parts of the world. For example, Cano et al. [30] found that agricultural waste, such as wood residues, is the most economically viable bio-resource in Ecuador, while Khan et al. [31] stated that animal manure is a more affordable bio-resource in Pakistan. Kasaeian et al. analyzed the effect of applying animal-based manure to produce biogas in Iran for a PV/Diesel/Bio hybrid system and found that a COE of 0.19 $/kWh can be achieved. However, this value can increase to 0.24 $/kWh under unfavorable economic conditions. As can be observed, the decision-making objectives in most of the previous literature primarily focus on economic goals. However, this approach can impact other sustainable development goals, including environmental considerations, energy efficiency, and the energy security of the HRES.

In the study of Guo et al. [32], six indexes were considered, including four economic, one technical, and one environmental objective. However, it was evident that the results of this study were significantly affected by the inclusion of more economic parameters. Edrisi et al. also stated that biomass could enhance the reliability indexes of HRESs and contribute to national sustainable development [33]. However, the environmental and economic aspects need further investigation. Das et al. [34] considered three economic, two technical, and one environmental objectives in their study on the integrated VIKOR-TOPSIS MCDM method for a standalone HRES integrated with green and non-green fueled generators. Their system demonstrated a COE of less than 0.16 $/kWh, a renewable fraction of over 95%, and a low unmet load. However, the study neglected investment reliability, energy security, and social objectives. In a similar study in India [35], considering investment reliability and life cycle assessment factors, the COE optimized at about 0.21 $/kWh, showing the importance of objective selection and weighting methods in MCDM. Song et al. [36] highlighted the significance of bio-energy in enhancing energy, environmental, economic, and social sustainability indexes, which are related to SDG1, SDG7, and SDG13 in China. While these results demonstrated the impact of bio-energy on the importance weight of energy system objectives, there is currently a lack of decision-making approaches that consider SDG-based MCDM in bio-based energy systems. Especially when the result of many studies such as Ref. [37] shows the possibility of between 10-40% affordable rural power supply by biomass resources. Therefore, it is necessary to pay more attention to catching up with the sustainable development scenario (SDS) outlined by the IEA, which calls for an annual increase of 6% in bioenergy [38]. Toopshekan et al. studied the optimization of a renewable-diesel CHP system and found that considering the importance of environmental factors in SDG17, estimating the objective importance of the MCDM method based on SDGs can result in an optimum system with a high renewable fraction but low power supply flexibility. This leads to excess electricity exceeding 50% and a cost of energy of more than 0.3 $/kWh [39]. Previous studies overlooked the potential for clean-fueled generators to align with SDGs when trying to maintain/improve the environmental, technical, reliability, and economic characteristics of HRESs.

Based on the conducted literature, the absence of sufficient attention given to biomass power in less developed countries, the prioritization of economic objectives in off-grid applications, the lack of a global framework for objective weighting in rural energy supply, and the challenges associated with decision-making for identifying the optimum power supply scenario considering all sustainable development goals are the main limitations. These limitations have not been simultaneously considered in previous research and represent a significant research gap for the optimization of stand-alone HRESs.

This study aims to harness the biomass potential, coupled with wind and solar energy, to propose a cost-effective and sustainable HRES that is more resilient to rural power supply. It takes advantage of the HOMER energy software and multicriteria decision-making, aligning with the sustainable development goals. The study targets the electricity supply for residential areas and the freshwater demand for two rural areas with different climate conditions in the southern and northern regions of Iran. The freshwater demand has been defined as a deferrable load to utilize the excess power from renewables and increase energy efficiency. Furthermore, the integration of bio and diesel generators has been applied to improve the reliability of the off-grid power supply and reduce the potential of CO_2 emissions. To address global warming and the SDGs by utilizing biomass, the TOPSIS method has been applied to the outputs of the HOMER tool. This method employs the primary objectives weighting method according to the SDG17 framework. Moreover, both agricultural and animal-based biomass, with different gasification ratios, have been considered to ensure accurate calculations of potential benefits by implementing biogas generators in a stand-alone HRES. Finally, a sensitivity analysis is performed to examine the impact of possible changes on the HRES, taking into account factors such as solar radiation, wind speed, and input prices.

2. Methodology

In sections 2.1 to 2.5, the power output formulation of wind turbines, photovoltaic panels, battery banks, fuel generators, and converters has been introduced. Also in section 2.6, the economic equations of HRES have been prepared.

2.1.Wind Turbine

HOMER data are updated at each time step, which is an hour here. Regarding wind turbines, the wind speed is calculated every hour at the hub height depending on the defined wind source as below [40]:

$$\mathrm{U}_{hub} = \mathrm{U}_{anem} \frac{\ln(Z_{hub}/Z_0)}{\ln(Z_{snem}/Z_0)} \tag{1}$$

In this equation U_{anem} (m/s) is the wind speed at anemometer height, Z_{hub} (m) is the height of the wind turbine's height, Z_0 (m) is the length of surface roughness, Z_{snem} (m) is the height of the anemometer. It is worth mentioning that the WT does not produce any energy when the wind speed is lower or higher than the so-called cut-in and cut-out wind speed respectively. Considering the wind speed at the hub height and the power curve of a wind turbine, the generated power by WT will be calculated at the standard condition. To achieve real condition, a density correction formula is used to reach the WT power output as follow [41]:

$$\mathrm{P}_{WTG} = \left(\frac{\rho}{\rho_0}\right) \mathrm{P}_{WTG,STP} \tag{2}$$

The generated power and air density at standard temperature and pressure are $P_{(WTG,\ STP)}$ (kW) and ρ_0 (kg/m^3) and the real air density is ρ(kg/m^3). The air density ratio (ρ/ρ_0) is computable by the ideal gas law.

$$\rho = \frac{P}{RT}, \tag{3}$$

$$\frac{\rho}{\rho_0} = \frac{P}{P_o}\frac{T_o}{T} \tag{4}$$

With the assumption that temperature declines linearly with gaining height up to 11000 m according to the US Standard Atmosphere, the air density is defined as [42]:

$$T = T_0 - Bz \quad (5)$$

$$\frac{\rho}{\rho_0} = \left(1 - \frac{Bz}{T_0}\right)^{g/RB} \left(\frac{T_0}{T_0 - Bz}\right) \quad (6)$$

In the above equations, T (K) is temperature, T_0 (K) is the temperature at standard condition, R (J/KgK) is the gas constant, P (Pa) is pressure, P_o (Pa) is the pressure at standard condition, B (K/m) is the lapse rate, z (m) is the altitude and g (m/s^2) is the gravitational acceleration.

2.2. Photovoltaic Panels

PV output power depends on weather conditions as well as temperature and technical parameters as shown in Eq. 7 [43]:

$$P_{PV} = Y_{PV} f_{PV} \left(\frac{\bar{G}_T}{\bar{G}_{T,STC}}\right)\left[1 \quad + \alpha_P\left(T_c - T_{c,STC}\right)\right] \quad (7)$$

where, Y_{PV}(kW), f_{PV}(%), $\bar{G}_T$(kW/m^2), $\bar{G}_{T,\ STC}$ (kW/m^2), α_P(%/(°C)), T_c(°C) and $T_{c,\ STC}$ (°C) are respectively, PV power generation at standard condition (rated capacity), derating factor of PV, solar radiation incident over the PV, the incident radiation of standard condition, temperature coefficient of power, the temperature of PV cell at each time step and standard condition. It should be noted that the adverse effect of temperature on PV output power [44] was considered in the calculations. The temperature of the PV cell is achievable by the energy balance equation indicated in Eq. 8 and solving the equation for cell temperature yields Eq. 9:

$$c\alpha G_T = \eta_c G_T + U_L(T_c - T_a) \quad (8)$$

$$\mathrm{T}_C = T_\alpha + G_T\left(\frac{\tau\alpha}{U_L}\right)\left(1 - \frac{\eta_c}{\tau\alpha}\right) \quad (9)$$

where τ(%) is the solar transmittance of PV cover, α(%) is the solar absorptance of PV, G_T(kW/m^2) is the solar radiation hitting PV, η_c(%) is the electrical efficiency of PV, U_L($kW/m^{2\circ}C$) is the heat transfer coefficient to the surrounding, T_c(°C) is PV temperature and T_a(°C) is the ambient temperature. For simplification, the nominal operating cell temperature (NOCT) is reported by manufacturers, which is the cell temperature with no load (η_c=0) at the nominal operating cell temperature of $T_{c,\ NOCT}$(°C), the incident radiation of $G_{T,\ NOCT}$=0.8(kW/m^2) and $T_{a,\ NOCT}$=20(°C) leading to the better form of the equation as Eq. 10:

$$T_C = T_\alpha + G_T\left(\frac{T_{c,NOCT} - T_{a,NOCT}}{G_{T,NNOCT}}\right)\left(1 - \frac{\eta_c}{\tau\alpha}\right). \qquad (10)$$

2.3.Battery Bank

Storage components play a crucial role in HRES by providing backup and mitigating intermittencies [45]. To effectively utilize excess renewable energy, it can be stored in storage banks, taking into consideration three limiting factors: the kinetic storage model, maximum charge rate, and the maximum charge current of the storage element [46]. The kinetic battery model (KBM) determines the maximum power that can be absorbed, yielding the following expression:

$$P_{batt,cmax,kbm} = \frac{kQ_1 e^{-k\Delta t} + Qkc\left(1 - e^{-k\Delta t}\right)}{1 - e^{-k\Delta t} + c\left(k\Delta t - 1 + e^{-k\Delta t}\right)} \qquad (11)$$

Then, the storage charge power according to the second constraint is:

$$P_{batt,cmax,mcr} = \frac{(1 - e^{-\alpha_c \Delta t})(Q_{max} - Q)}{\Delta t} \qquad (12)$$

Finally, the maximum power related to the maximum charge current is:

$$P_{batt,cmax,mcc} = \frac{N_{batt} I_{max} V_{nom}}{1000} \qquad (13)$$

In the above equations, the accessible energy in the beginning is Q_1(kWh), the total energy in the beginning is Q(kWh), the ratio of storage capacity is c, the storage rate constant is k(h^{-1}), the time step length is Δt(h), the maximum charge rate of storage is α_c(A/Ah), the total capacity of the storage unit is Q_{max}(kWh), the batteries' number in the storage unit is N_{batt} and the nominal voltage of the batteries is V_{nom}(V). Then, the maximum storage is determined by choosing the least amount of the above-mentioned values.

$$P_{batt,cmax} = \frac{MIN\left(P_{batt,cmax,kbm},\ P_{batt,cmax,mcr},\ P_{batt,cmax,mcc}\right)}{\eta_{batt,c}} \qquad (14)$$

The efficiency of battery charging ($\eta_{batt,c}$) and battery discharging ($\eta_{batt,d}$) is calculated by the root of battery round-trip efficiency ($\eta_{batt,rt}^{0.5}$). Round-trip efficiency ($\eta_{batt,\ rt}$) is the amount of energy that could be restored from the energy put into the storage bank. The maximum discharge power over a definite time could be reached with the kinetic storage model as:

$$P_{batt,dmax,kbm} = \frac{-kQ_{max} + kQ_1 e^{-k\Delta t} + Qkc(1 - e^{-k\Delta t})}{1 - e^{-k\Delta t} + c(k\Delta t - 1 + e^{-k\Delta t})} \quad (15)$$

With the consideration of discharging loss ratio ($\eta_{batt,d}$), the maximum discharge power is:

$$P_{batt,dmax} = \eta_{batt,d} P_{batt,dmax,kbm} \quad (16)$$

2.4. Gasifier and Fuel Generator

Biomass, due to the abundance of waste crops, livestock, and forests in rural areas, serves as an easily accessible energy source. Its utilization can effectively address the intermittency challenges in HRESs [47], and increase the resilience and sustainability of the system [48]. Furthermore, the gasification of animal waste is environmentally beneficial as it inhibits the production of methane gas during storage [49]. If the biomass is in its raw form, it needs to undergo a gasification and thermochemical process to convert it into biogas, which can then be used as fuel. The resulting gas, known as syngas, has a lower heating value compared to fossil fuels but offers higher efficiency, increased control, and reduced emissions. The amount of biogas generated from biomass (m^3) is determined by multiplying the gasification ratio ($kg_{gas}/kg_{biomass}$) and the biomass feedstock per day (kg/day) [50]. Alternatively, the power generated by the biogas generator could be defined as [51]:

$$P_e = \eta_e Q_{bg} LHV_{bg}, \quad (17)$$

$$LHV_{bg} = \frac{P_{CH_4}}{100} LHV_{CH_4} \quad (18)$$

Here, the efficiency of electrical conversion is η_e, the biogas flow rate is Q_{bg} (m^3/h), the available methane in the biogas is P_{CH_4}(%), the lower heating values of biogas and methane are LHV_{bg} and LHV_{CH_4}. LHV_{bg} can be calculated based on LHV_{CH_4}. The LHV typically has a value ranging from 15 to 25 MJ/m^3 for various organic substances. However, for methane specifically, the LHV is approximately 36.3 MJ/m^3 [51]. The generator output power (P_{FG}) and its fuel consumption (F_{FG}) can be calculated by Fq. 19 and Eq. 20. where η_{FG} (%) refers to fuel generator internal efficiency, Y_{FG} (kW) is the nominal power of fuel generator device, and a and b are the constant multipliers of generator announced by manufacturer. Furthermore, the diesel fuel emission is about 2.6 kg/L [52] while biogas emission is less than 5% of this value.

$$P_{FG} = F_{FG}.\eta_{FG}.LHV_{Fuel} \quad (19)$$

$$F_{FG}(\mathrm{t}) = a.Y_{FG} + b.P(t) \quad (20)$$

2.5.Converter

The converter is used to link the AC and DC power hub containing an inverter and rectifier that could convert DC to AC and AC to DC electricity respectively. The output power of the converter is a function of the inverter (η_{inv}) and rectifier (η_{rec}) efficiency [53].

$$\mathrm{P}_{inv,out} = \eta_{inv}\mathrm{P}_{DC} \quad (21)$$

$$\mathrm{P}_{rec,out} = \eta_{rec}\mathrm{P}_{AC} \quad (22)$$

2.6. Economic Affairs

The cost of energy (COE) in $/kWh as one of the significant parameters to compare various systems equals the division of annualized cost ($/year) to the total electrical load served (kWh/year) [54].

$$COE = \frac{C_{ann,tot}}{E_{served}} \quad (23)$$

The annualized cost is computable with net present cost (NPC) in $, which is the value of lifetime revenues deduced from the price of installing and operating components a present [55].

$$C_{ann} = CRF(i,R) * NPC \quad (24)$$

where R is the lifetime of the project (year) and the capital recovery factor (CRF) is:

$$CRF(i,R) = \frac{i(1+i)^R}{(1+i)^R-1}. \quad (25)$$

The annual discount rate of i could be determined as [56]:

$$i = \frac{i^{\circ} - f}{1+f} \quad (26)$$

In the present study the annual inflation rate, nominal discount rate, project lifetime, diesel fuel price, and the maximum annual capacity shortage are considered 15%, 18%, 20 years, 0.3 $/L, and 1%, respectively.

3. System Modeling and Input Data

The HOMER (Hybrid Optimization Model for Electric Renewable) software, developed by the National Renewable Energy Laboratory (NREL), has been widely utilized in various on-grid or off-grid research and has been subjected to experimental validation [57], numerical verification, and validation using well-known optimization codes. Moreover, it is considered one of the most accessible tools for investors and policymakers to analyze the economic aspects of renewable energy systems. The schematic representation of the analyzed HRES's overall configuration can be seen in Figure 1. Also, the Cycle Charging and Load Following dispatch strategies are conducted to control the renewable energy systems in the optimization problem. dispatch strategies play a critical role in controlling renewable energy systems, and they involve determining the optimal use of available energy resources to meet the energy demand at any given time. Cycle charging dispatch is a strategy used to maximize the use of generators when they are turned on, particularly in systems that integrated with high intermittent renewable energy sources. It is worth noting that the Cycle charging dispatch strategy was selected as the controlling mechanism because this strategy is similar to the performance of generators in local rural areas. In this strategy, the generator is turned on at its maximum capacity, enabling it to charge the battery bank using its surplus power generation. Therefore, non-renewable sources also participate in the process of charging the batteries, and the lack of experts to manage the level of fuel input to the generator in remote areas will not be a challenge.

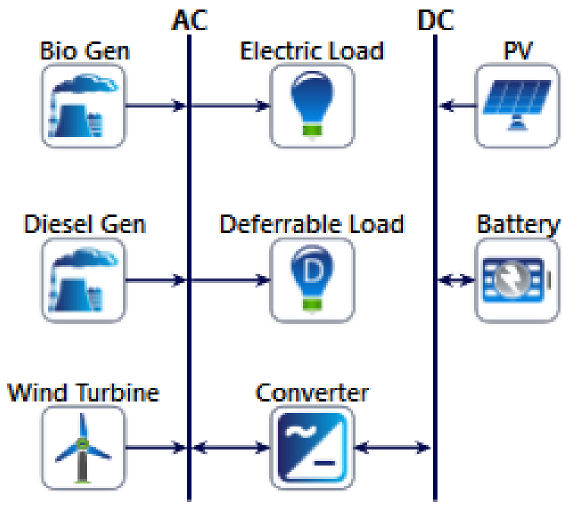

Fig. 1 Schematic illustration of the proposed multi-generation renewable energy system

3.1. Case Studies

Iran benefits from high levels of solar irradiation, wind speeds, and agricultural or livestock residue production. In this study, two deprived and remote regions, namely Kavat and Azad (Figure 2), are modeled to provide electricity for basic necessities and freshwater through standalone HRES.

Fig. 2 Kavat and Azad map locations.

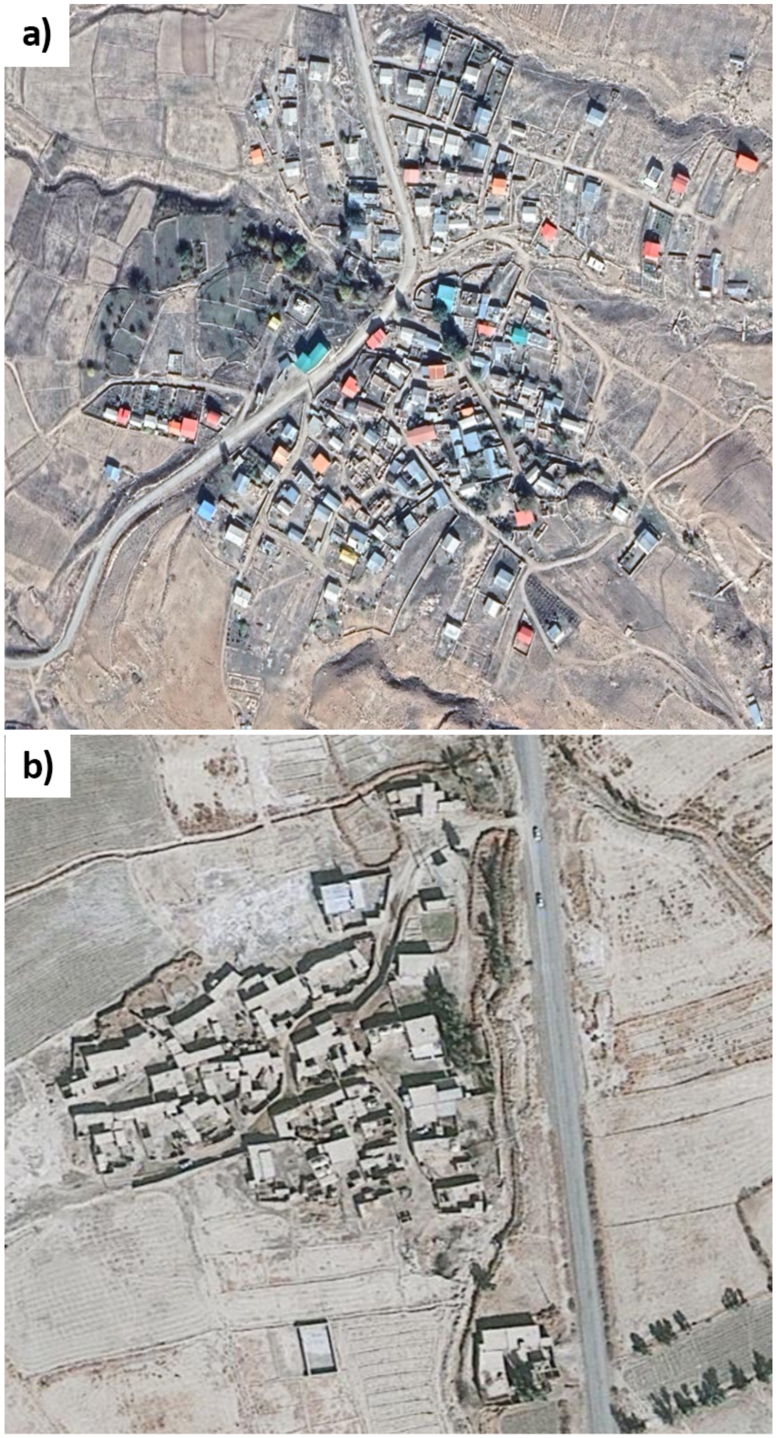

Fig. 3 Close satellite view of a) Kavat village and b) Azad village [59].

The locations of the two areas, Kavat and Azad, can be observed in Figure 3, as they experience different conditions. Kavat is one of the oldest villages in Mazandaran province (mild and humid climate) in the North of Iran with a latitude of 36.278°, a longitude of 53.817°, and an altitude of

1587m. Azad is located in the Sistan and Baluchestan province (warm and dry climate) in the East of Iran at a latitude of 31.104°, a longitude of 61.799°, and an altitude of $483m$. In the past few decades, the resident population of Kavat and Azad has been declining primarily due to factors such as limited job opportunities, inadequate freshwater supply, lack of development, and low wages. Specifically, between 2011 and 2016, the population of Kavat decreased from 339 to 227 individuals in 96 to 81 families, while the population of Azad decreased from 172 to 101 individuals in 45 to 36 families [58]. The majority of the population in these areas depends on agriculture and animal husbandry for their livelihoods. These statistics highlight the pressing need for improved facilities, attention, and development to address and potentially reverse this concerning trend of emigration.

3.2. Loads

The average electricity consumption in Kavat is 510.3 kWh/day, with a peak demand of 108.4 kW. In Azad, the average consumption is 244.8 kWh/day, with a peak demand of 52 kW. Figure 4 provides a visual representation of the hourly electricity demands per rural household in Iran. It demonstrates that higher loads occur during the warmer months (June to September), while lower loads are observed from December to February, reflecting seasonal variations. When renewable resources are abundant, demand is low, and storage banks are full, the installed renewable capacity can lead to excess electricity generation. This excess is due to the goal of ensuring the highest power supply reliability even under the most challenging conditions [60]. To efficiently utilize a portion of the surplus power and meet essential local needs, a desalination device is integrated with the HRES. Therefore, it is intended that freshwater be supplied through reverse-osmosis desalination (ROD), assuming each human would consume approximately 25 L/day. In other words, considering 0.025 m^3 as the minimum needed daily freshwater for each person, Kavat and Azad would require 5.7 m^3 and 2.5 m^3 per day, respectively. The desalination operation for generating 1 m^3 of freshwater through ROD requires an average of 3.7 kWh [61,62]. It should be noted that freshwater can be produced at any time of the day, stored in a tank, and used during the day. Therefore, the power required for this process can be classified as a deferrable load, meaning that the exact timing is not a priority, and the process can be carried out when excess energy is available. The maximum power requirement is equivalent to that of two 0.8 kW pumps, which represents the peak load necessary for delivering water to the storage tank and through the ROD system.

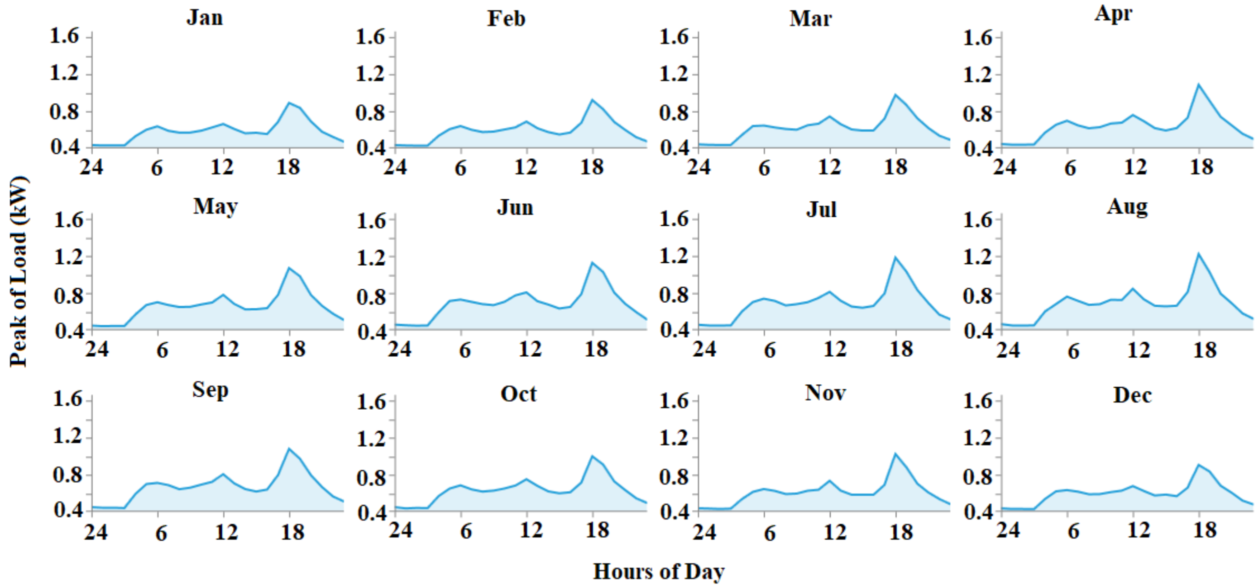

Fig. 4 Power consumption profile per rural household.

3.3. Solar and Wind Potential

Iran's location in the radiation belt of the Earth makes it an ideal location for receiving solar radiation. In fact, more than 50% of Iran enjoys over 5 kWh/m^2/day of radiation [44]. Figure 5 shows the average global horizontal irradiance (GHI) and average wind speed for each month in Kavat and Azad, based on NASA meteorological data. The radiation is highest in the summer months and lowest in winter. Generally, Azad receives more radiation due to its location in the southern part of Iran compared to Kavat in the northern part. Furthermore, since Kavat is located at a higher altitude (1587 m), it enjoys a larger amount of wind speed, reaching 4.1 m/s, compared to Azad. Table 1 and Table 2 represent the economic and technical characteristics of the selected PV panel and wind turbine, respectively, which are prevalent in Iranian markets.

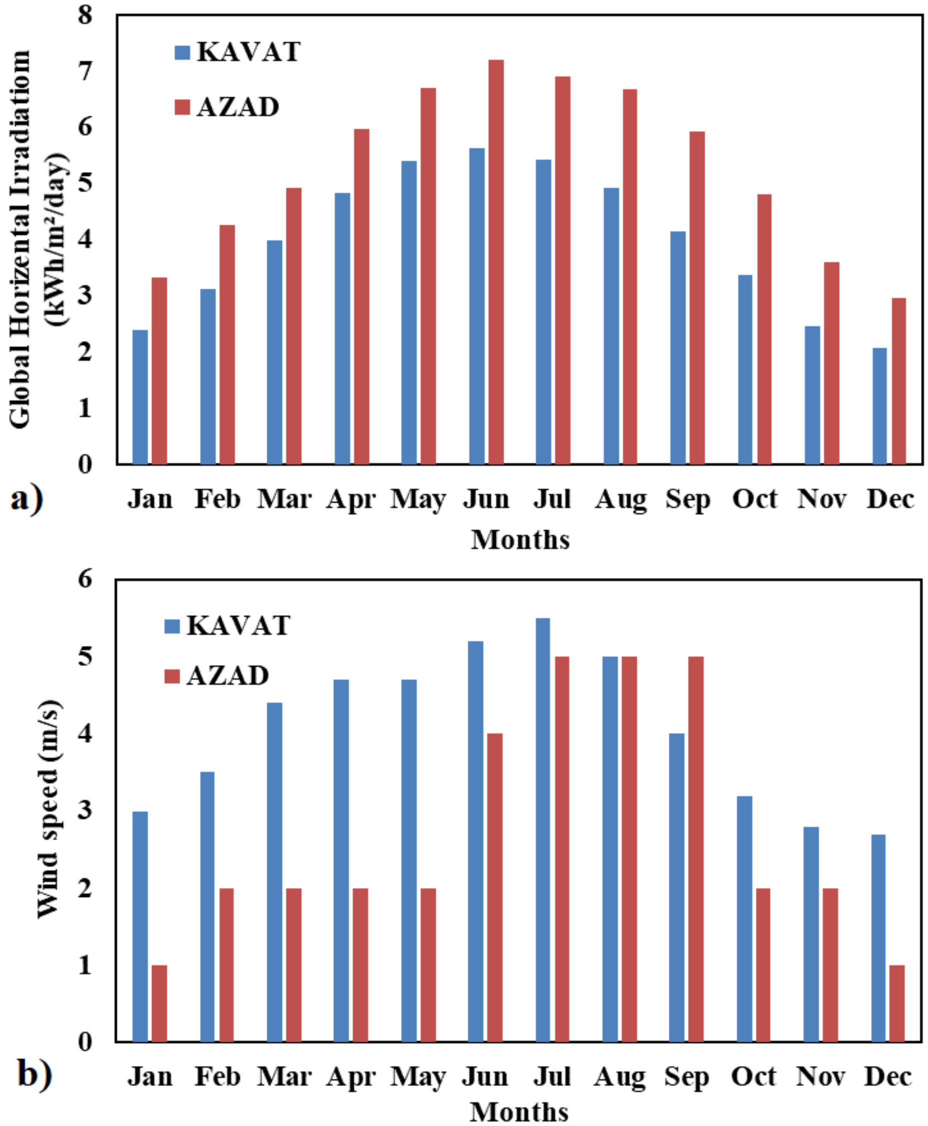

Fig. 5 Local solar and wind potential: a) Monthly average global horizontal irradiation and b) Monthly average wind speed [63].

Table 1. The techno-economic properties of sharp ND-250QCS PV module [6].

Specification	Value
Maximum Power	250 W
Nominal operation cell temperature	47.5 °C
Short Circuit Current	8.90 A
Open Circuit Voltage	38.3 V
Temperature Coefficient	-0.458%/C

Efficiency	15.30%
Lifetime	20 Years
Capital Cost	1400 $/kW
Replacement Cost	1400 $/kW
Maintenance Cost	20 $/kW/Year

Table 2. Wind turbine specifications [61].

Specification	Value
Type	Horizontal
Rated Power	1.5 kW
Power Coefficient	0.45
Rotor Diameter	3.2 m
Hub Height	12 m
Cut-in and Cut-off Speed	2.2 m/s
Cut-out and Cut-off Speed	12 m/s
Lifetime	20 Years
Capital Cost	3000 $/kW
Replacement Cost	2700 $/kW
Maintenance Cost	30 $/Unit/Year

3.4. Biomass Potential and Fuel Generators

Biogas is generated by the fermentation of organic elements in biomass. These materials mainly consist of carbon dioxide (CO_2) and methane (CH_4) obtained from crop residue, sewage, industrial or household waste, and animal dung [16]. The highest share of biomass is allocated to agricultural residue, followed by livestock waste, with 59% and 28% in the world biogas production [64]. Agriculture is common in the northern regions of Iran and animal husbandry is common in the southern regions of Iran, so these regions have suitable conditions for using the biomass potential.

Animal breeding, such as cattle and sheep, is a major occupation in rural areas, which can provide accessible and biodegradable biomass. Daily sheep droppings amount to almost 2 kg/day, and dairy cow dung contributes roughly 12 kg/day of solid waste [50]. On average, each household in

Azad village keeps 2 cattle and 11 sheep, resulting in the production of nearly 1.5 tons/day of animal manure, considering a 20% loss in waste collection operations. The collection and delivery of biomass to the site can cost about $10/ton. It is achievable to generate nearly 0.04 m^3 of biogas from 1 kg of manure, containing 50-70% CH_4 (the remaining being mostly CO_2), with a lower heating value (LHV) between 21 and 24 MJ/m^3 [65]. For the production of biogas from biomass, an LHV of 23 MJ/m^3, a gasification ratio of 0.7, a generator capital and replacement cost of 1500 $/kW [66] with a maintenance cost of 0.07 $/hour/kW, and a lifetime of 15000 hours are considered. While the total capital and O&M cost of a diesel generator is almost half that of a bio-generator due to its lower complexity.

Due to the abundance of fields in rural districts, agriculture is also prevalent and assumed to be one of the main sources of rural income. In Iran, agricultural residues account for nearly 30% of the total crop, including transportation and harvesting [67]. However, these agricultural wastes are usually burnt at a rate of 80% in Iran, causing environmental and ecological issues. The prominent farming practice in Mazandaran is rice cultivation, while in Sistan and Baluchestan, it is Alfalfa [68] with a residue-to-crop ratio (RCR) of 1.75 [69] and 0.15 [70] respectively. Based on the average amount of crop/rice production and considering 30% waste, Kavat has the potential of producing 630 kg of agricultural waste. Table 3 presents the available biomass characteristics in the selected cases.

Table 3. Biomass resource characteristics in the selected cases.

Bio resource	**LHV (MJ/kg)**	**Carbon content (%)**	**Gasification Ratio (m^3/kg_{mass})**	**Estimated Average Price ($/ton)**	**Estimated Availability (ton/day)**	**Case village**
Animal-based [50,71]	5.50	5.00	0.04-0.07	10	1.70	Azad
Agriculture-based [71,72]	4.40	5.00	0.11-0.16	20	0.63	Kavat

3.5. Air Temperature

The monthly consumption of fresh water and the efficiency of PV is related to the ambient temperature. PV works better and generates more power when kept at lower temperatures. It is also estimated that there will be harsher conditions between 2025 and 2049, especially in the southern part of Iran [73], affirmed by the monthly average temperature of Azad and Kavat in Fig. 6. As can be seen, the southern part of Iran, has experienced higher air temperatures than the northern part.

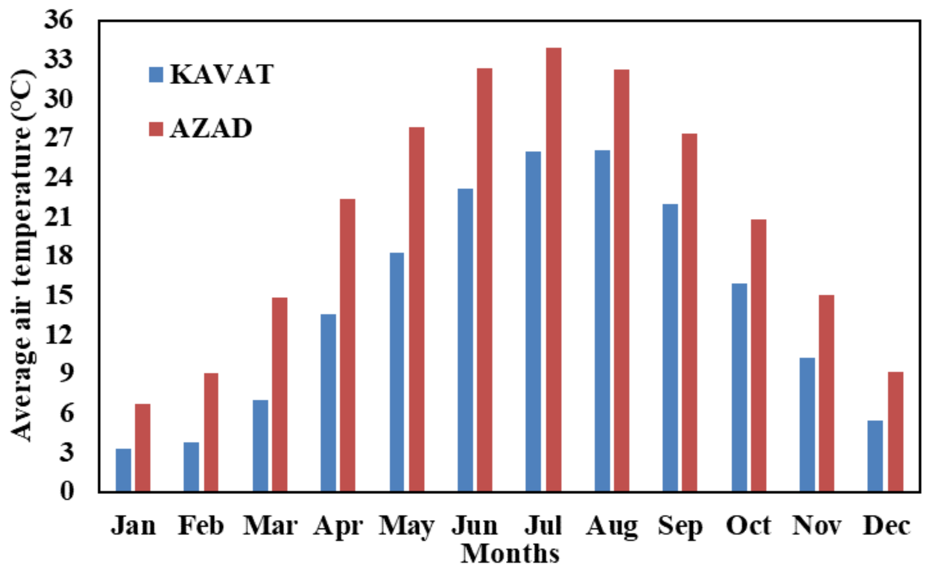

Fig. 6 Monthly average ambient temperature [63].

3.6. Storage Bank and Converter

Batteries play a pivotal role in not only overcoming the intermittency of renewable energy but also storing excess energy to be used at low-demand times. It also enhances the system's efficiency and avoids exhausting costs, especially at peak demands. Table 4 shows the specifications of the 1 kWh Li-Ion battery utilized and also the generic converter used in the simulation process.

Table 4. The economic and technical properties of storage banks and the power converter [74].

Characteristics	**Data**
Generic 1kWh Li-Ion Battery bank	
Battery lifetime	15000 h
Nominal Capacity	167 Ah
Roundtrip efficiency	90%
Maximum Charge Current	167 A

Capital cost	500 $/unit
Nominal Voltage	6 V
O&M Cost	1% capital $/year
Replacement Cost	500 $/unit
Generic 1kW Power Converter	
Converter Lifetime	12 years
Rectifier Efficiency	95%
Inverter Efficiency	95%
O&M Cost	1% capital $/year
Capital Cost	300 $/kW
Replacement Cost	300 $/kW

4. Primary Model Validation

A comparison of HOMER's accuracy in the field of renewable energy systems with other common methods has demonstrated the tool's significant potential. In a review study, Emad et al. [75], highlighted the favorable competitiveness of HOMER's results when compared to GA (genetic algorithm) and PSO (particle swarm optimization). Additionally, Ref. [76], demonstrated that HOMER is the most widely used pre-made software in academic renewable energy optimization studies due to its attractive accuracy and optimization speed compared to other tools in this field.

Previously, Fodhil et al. [77] and Yu et al. [78] validated the output of HOMER using PSO and Adaptive Marine Predators Algorithm (AMPA), respectively. However, to ensure the reliability of the simulation results, the initial model was validated using a similar study that applied a coded optimization algorithm. For the validation of the primary model with well-known optimization algorithms, the input data from Singh et al. [79] was imported into the HOMER software to compare the output results with the Particle Swarm Optimization (PSO) algorithm. As observed in Table 5, the results are nearly similar, with a slight variation in NPC and COE. This discrepancy may be attributed to the difference in the focus factor between the two models. In the HOMER simulation, a focus factor of 5% (indicating high reliability) was employed.

Table 5. Validation of applying the HOMER optimizer with the results of [79] for a similar configuration

Algorithm	PV (kW)	WT (kW)	BG (kW)	BES (kWh)	Conv (kW)	RF (%)	NPC (K$)	COE ($/kWh)
PSO [79]	251	20	43	1400	115	100	730.1	0.17
HOMER	275	19	45	1350	115	100	748.2	0.18

5. Multi-criteria Decision Making (MCDM)

The main problem with the HOMER software is that decision-making is based on a single objective criterion (NPC). However, in order to choose the best HRES, it is necessary to consider a set of criteria [80]. As shown in Table 6, these criteria are also reflected in the global sustainable development goals. Therefore, the outputs of the HOMER software were categorized, and multi-criteria decision-making is performed using the TOPSIS (Technique for Order Preference by Similarity to the Ideal Solution) method in MATLAB software to determine the optimal HRES. To accurately estimate the optimal scenario, the decision objectives must be weighted. In this study, two weighting methods for the selected variables have been used. In the first method, based on the results of Sedghiyan et al. [81], the weight of each parameter is estimated using the AHP (Analytic Hierarchy Process) method in Iran. In the second method, each of the selected objectives was innovatively weighted based on the number of SDGs related to the parameters involved in each objective. In the first step, the ratio of the total number of SDGs in each objective to the total number of SDGs related to all objectives is calculated, and then this number is divided by the total number of parameters in each objective (Table 6). The constant worldwide framework of SDG17 leads to different weights for each objective, while the parameters in each objective reflect similar weights in this study. In this method, the weight changes in the scale of parameters can be adjusted based on local policy, prioritizations of energy-related national organizations, and long-term programs, which vary in each city. Equations 27 to 40 state the TOPSIS formulas, presenting the MATLAB codes in Appendix A [82].

Table 6. Elected objectives and weighted values of each decision-making parameters for the MCDM process.

Objective	**Decision-Making Parameters**	**Related SDGs to the Objectives**	**SDG Weights**	**AHP Weights**
Economic	NPC (Net Present Cost) IC (Initial Cost) COE (Cost of Energy)	Sustainable cities in SDG11 Economic growth in SDG8 Affordable energy in SDG7 No poverty in SDG1	9.5%	12%
Environmental	NO_X (Nitrogen Oxides) CO_2 (Carbon Dioxide)	Life on land in SDG15 Climate action in SDG13 Clean energy in SDG7 Good health in SDG3	14.2%	13%
Energy Security	Fuel Dependency (FD) Diversity	Responsible production in SDG12 Sustainable cities and communities in SDG11 Reduced inequalities in SDG10	10.7%	8.5%
Technical	EX_{EL} in (Excess Electricity) Local Resources Share (LRS) Unmet Load (U_{Load})	Responsible production in SDG12 Sustainable cities in SDG11 Energy infrastructure in SDG9	7.2%	7.5%

The i and j signs in Eq. 1 specify the number of criteria and the number of alternatives, respectively. Furthermore, when estimating the weight of parameters based on SDG goals, Eq. 28 is utilized to determine the weight of parameters in each decision-making objective. Where $N_{SDG,C}$ is the number of related SDGs for the selected decision-making objective, $N_{SDG,T}$ denotes the total number of SDGs related to all objectives. Meanwhile, $N_{P,C}$ indicates the number of decision-making parameters in the selected objective.

$$i = 1,2,3, \dots m \quad and \quad j = 1,2,3, \dots, n \tag{27}$$

$$W = \frac{N_{SDG,C}}{N_{SDG,T} \times N_{P,C}} \tag{28}$$

The optimization algorithm can have negative or positive criteria or objective functions. Additionally, each optimized scenario introduces an alternative. Equation 2 defines the necessary criteria and alternatives for both the weight matrix (W) and the decision matrix (X). Accordingly, the normalized matrix (Eq. 30) is created. Finally, the normalized version of the weighted matrix is calculated by Eqs. 31 and 32.

$$X = \{x_{ij}\} \quad and \quad W = [w_i] \tag{29}$$

$$N_{ij} = \frac{x_{ij}}{\sum_{i=1}^{m} x_{ij}} \tag{30}$$

$$R = \frac{x_{ij}}{\left(\sum_{i=1}^{m} x_{ij}^2\right)^{0.5}} \tag{31}$$

$$V = R \times W \tag{32}$$

In the next step, the positive and negative ideal solutions are estimated based on Eq. 33 and Eq. 34, respectively. It should be noted that in Table 6, the local resources shares and diversity parameters are positive criteria while other factors are negative criteria. Eqs 35 and 36 are applied to calculate the comparative proximity of every acquired solution to the optimal solution. Finally, the closeness coefficient is estimated based on Eq. 37, where a higher coefficient showed better optimality of the HRES scenario due to the SDG17 framework.

$$A^{+} = (v_1^{+}, \dots, v_m^{+}) = \{(max\ V |\ positive\ criteria), (min\ V |\ negative\ criteria)\} \tag{33}$$

$$A^{-} = (v_1^{-}, \dots, v_m^{-}) = \{(min\ V |\ positive\ criteria), (max\ V |\ negative\ criteria)\} \tag{34}$$

$$S^{+} = \sqrt{\sum_{i=1}^{m} \left(v^{+} - v_{ij}\right)^2} \tag{35}$$

$$S^{-} = \sqrt{\sum_{i=1}^{m} \left(v^{-} - v_{ij}\right)^2} \tag{36}$$

$$C_j = \frac{S^{-}}{S^{-} + S^{+}}; 0 \le C_j \le 1, for\ j = 1,2, \dots, n \tag{37}$$

6. Results and Discussion

In this part, first, the overall optimization results of the HOMER software, categorized based on NPC, are introduced. Then, the outputs of the TOPSIS method are stated to take advantage of the multi-criteria solution finding process based on the SDG framework. After finding the optimum scenario, the power supply and technical performance are discussed. Then, a sensitivity analysis of the most important variables of the proposed hybrid energy system is performed. Finally, a comprehensive discussion and comparative analysis are conducted in the last subsection.

6.1. HOMER Output Results

The outputs of the HOMER results in Tables 7 and 9 demonstrate that the optimum configuration from an economic point of view is PV/WT/BIO/DG/BAT with a COE of 0.218 $/kWh for Kavat and PV/BIO/DG/BAT with a COE of 0.200 $/kWh for Azad. As it is obvious, the main reason for the difference in the optimum hybrid configuration is rooted in the wind potential of Kavat compared to Azad village. In Azad, the maximum installation of one wind turbine is observed, while in Kavat, the installation of 28 wind turbines is observed in the optimum scenario. On the other hand, due to very good solar radiation in Azad, the optimum PV capacity is about 70 kW, while in Kavat, it is about 32 kW. The lower capital cost of PV compared to WT and the high potential of the solar resource compared to wind potential in Iran result in a lower cost of energy in the southern village than in the northern village. Another key point is the role of fuel generators in improving the economic affordability of the hybrid system. As can be seen, the removal of the diesel generator from the optimum scenario will increase the energy costs for Kavat and Azad by 15% and 9% respectively. Additionally, applying bio generators based on the local bio potential improves energy costs by 9% and 7% respectively.

By referring to Table 8, it can be observed that applying a bio generator along with a diesel generator in the HRES reduced annual CO_2 emissions by about 30% compared to a diesel-based HRES. On the other hand, based on Table 10, when renewable energy production in the night hours is low due to the system's dependency on PVs, this approach can't significantly reduce emissions. The main reason is the lower cost of power generated by diesel fuel compared to biofuel, which results in a large amount of power being supplied by diesel fuel during night hours.

All proposed scenarios have less than 1% (<80 hours) unmet load, demonstrating the proper power supply reliability of the hybrid units. Furthermore, the optimum scenarios have a renewable fraction of more than 70%, making the hybrid system an environmentally friendly unit. However, as can be seen from Table 7 to Table 10, the economically optimal scenario does not yield the best environmental, technical, and energy security results. This highlights the importance of multi-criteria decision-making for each of the selected cases.

In hybrid renewable energy systems, energy efficiency is defined as the portion of useful generated electricity to the total generated power. Useful electricity refers to the generated power by the hybrid system that is used to supply load or be stored in storage banks, while the total generated power also includes the unused part of power. Therefore, the difference in energy efficiency in each scenario is highly dependent on the unused part of electricity, which is known as excess electricity. Accordingly, a lower excess electricity percentage (EX_{EL}) indicates a higher total energy efficiency of the power supply process. As seen in Tables 8 and 10, a higher share of fuel generators compared to the PV/WT system can lead to lower excess electricity due to increased power supply flexibility. However, more operating hours for the diesel generator can result in higher emissions from the HRES. In contrast, the operation of a bio generator, which is a flexible near-zero pollutant technology, can lead to lower emissions while improving the energy efficiency of a stand-alone microgrid.

Table 7. Techno-economic optimization results of HOMER software for Kavat village.

Scenario	**PV (kW)**	**WT (Unit)**	**BIO (kW)**	**DG (kW)**	**BAT (kWh)**	**COE ($/kWh)**	**NPC ($)**	**IC ($)**
PV/WT/BIO/DG/BAT	70.3	28	15	10	145	0.218	651,322	309,116
PV/./BIO/DG/BAT	95	-	15	15	127	0.224	666,524	254,738
PV/WT/./DG/BAT	84.9	35	-	15	219	0.240	714,194	376,145
PV/WT/BIO/./BAT	143	37	15	-	374	0.251	746,174	544,494
./WT/BIO/DG/BAT	-	64	15	15	135	0.256	761,154	317,419
PV/./ ./DG/BAT	170	-	-	15	319	0.270	803,978	444,917
PV/./BIO/./BAT	246	-	15	-	486	0.274	812,966	636,906
PV/WT/./ ./BAT	293	59	-	-	635	0.374	1,110,000	932,380
PV/./ ./ ./BAT	474	-	-	-	706	0.408	1,210,000	1,050,000

./WT/./DG/BAT	-	147	-	15	856	0.452	1,340,000	908,772
./WT/BIO/./BAT	-	180	15	-	853	0.473	1,410,000	1,010,000
./WT/././BAT	-	518	-	-	1472	0.978	2,900,000	2,330,000

Table 8. Techno-enviro-security optimization results of HOMER software for Kavat village.

Scenario	**CO_2 (kg/yr)**	**NO_X (kg/yr)**	**EX_{EL} (%)**	**U_{Load} (%)**	**LRS (%)**	**diversity**	**FD (L/yr)**
PV/WT/BIO/DG/BAT	36,160	212	13.3	0.573	76.6	5	13,801
PV/./BIO/DG/BAT	45,303	266	18.9	0.578	70.7	4	17,291
PV/WT/./DG/BAT	65,876	386	18.7	0.611	57.3	4	25,164
PV/WT/BIO/./BAT	20.8	0.145	26.8	0.617	100	4	0
./WT/BIO/DG/BAT	44,179	259	5.38	0.559	71.4	4	16,860
PV/././DG/BAT	68,954	405	36.2	0.350	55.5	3	26,340
PV/./BIO/./BAT	14.3	0.0989	41.7	0.740	100	3	0
PV/WT/././BAT	0	0	57.6	0.756	100	3	0
PV/./././BAT	0	0	67.5	0.724	100	2	0
./WT/./DG/BAT	44,150	259	21.9	0.619	71.4	3	16,865
./WT/BIO/./BAT	26.6	0.184	30.5	0.593	100	3	0
./WT/././BAT	0	0	71.9	0.887	100	2	0

Table 9. Techno-economic optimization results of HOMER software for Azad village.

Scenario	**PV (kW)**	**WT (Unit)**	**BIO (kW)**	**DG (kW)**	**BAT (kWh)**	**COE ($/kWh)**	**NPC ($)**	**IC ($)**
PV/./BIO/DG/BAT	32	-	10	5	58	0.200	284,836	102,615
PV/WT/BIO/DG/BAT	33	1	10	5	57	0.201	286,555	106,580
PV/././DG/BAT	62.5	-	-	15	184	0.215	305,429	208,189
PV/WT/./DG/BAT	61.5	1	-	15	179	0.215	306,588	206,629
PV/./BIO/./BAT	72.7	-	10	-	223	0.218	309,675	237,564
PV/WT/BIO/./BAT	37	1	10	-	104	0.219	312,123	129,240
././DG/BIO/BAT	-	-	10	15	27	0.255	363,359	53,048
./WT/BIO/DG/BAT	-	1	10	15	24	0.256	363,875	54,542
PV/./././BAT	123	-	-	-	255	0.264	374,830	313,138

PV/WT/./../BAT	121	1	-	-	255	0.265	376,506	314,351
./././BIO/BAT	-	-	-	15	83	0.298	423,202	70,825
./WT/./BIO/BAT	-	1	-	15	91	0.299	426,074	76,853

Table 10. Techno-enviro-security optimization results of HOMER software for Azad village.

Scenario	**CO_2 (kg/yr)**	**NO_X (kg/yr)**	**EX_{EL} (%)**	**U_{Load} (%)**	**LRS (%)**	**diversity**	**FD (L/yr)**
PV/./BIO/DG/BAT	17,025	99.9	11.4	0.587	77	4	6,488
PV/WT/BIO/DG/BAT	16,686	97.9	12.7	0.540	77.5	5	6,358
PV/././DG/BAT	13,290	78	18.5	0.563	82.9	3	5,077
PV/WT/./DG/BAT	13,569	79.6	17.7	0.575	82.6	4	5,183
PV/./BIO/./BAT	8.39	0.0582	22.6	0.635	100	3	0
PV/WT/BIO/./BAT	61.8	0.429	13.4	0.573	100	4	0
././DG/BIO/BAT	37,110	218	0	0.561	49.9	3	14,153
./WT/BIO/DG/BAT	35,539	209	0	0.546	52.1	4	13,552
PV/././BAT	0	0	51.3	0.690	100	2	0
PV/WT/././BAT	0	0	51	0.694	100	3	0
./././BIO/BAT	77,626	455	0.638	0	0	2	29,652
./WT/./BIO/BAT	77,150	453	0	0.550	0	3	29,471

Figure 7 shows the monthly power generation share of each component in the HOMER's optimal scenario. Approximately, the overall energy production is about 230,981 kWh/yr for Kavat. In this village, the share of PV, BG, DG, and WT is about 22.2%, 21.4%, 19.5%, and 16.9%, respectively. The marginal power generation cost of each component is about 0.065, 0.067, 0.081, and 0.161 $/kWh, respectively. Furthermore, the battery bank has an annual power discharge of 27,389 kWh with an average energy cost of about 0.062 $/kWh. The total energy production in Azad is about 108,497 kWh/yr with a share of 50.5%, 30%, and 19.5% for PV, BG, and DG, respectively. In this village, the marginal power generation cost of PV is reduced to about 0.053 $/kWh due to appropriate solar potential. Also, the battery bank has an 11,988 kWh annual power discharge with an average energy cost of about 0.072 $/kWh. Although the energy cost of biogas generators in the northern and southern parts of Iran showed a negligible difference of less than 0.004, there was a significant difference of approximately 10% and 30% in the energy costs of PV and WT, respectively. Consequently, biomass proves to be a reliable resource that contributes to stabilizing and enhancing the attractiveness of hybrid renewable energy systems.

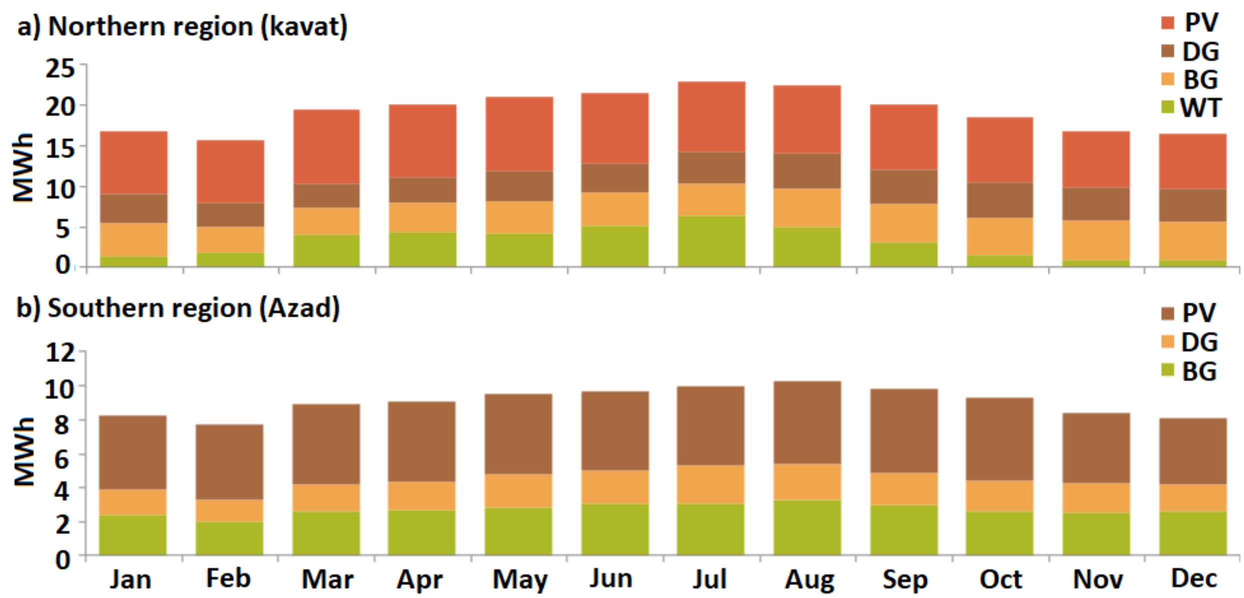

Fig. 7 Monthly electrical production share of each component in the HOMER's optimum scenario for a) Kavat and b) Azad.

6.2. *Optimal Configuration by MCDM*

By incorporating the estimated decision-making parameter weights, based on the AHP and SDG17 framework, into the TOPSIS method, the order of preference for optimum scenarios has changed compared to the results obtained from HOMER. According to Figure 8, the PV/WT/Bio/battery configuration is selected by the MCDM in Kavat and Azad, resulting in a COE of about 0.25 and 0.22 $/kWh, respectively. This configuration relies 100% on local resources and supplies power with near-zero emissions. The maximum possible power outage in this scenario is less than 50 hours per year, demonstrating a significant improvement compared to the primary HOMER output for the selected rural cases. In this configuration, the power supply is accomplished using four different power equipment without any reliance on rural fossil fuels, providing higher energy security compared to the government's current choice of pure DG power supply for remote areas.

However, the only drawback of this scenario is the presence of more than 10% excess electricity, which is a result of its heavy reliance on renewable sources during peak demand periods.

It is important to note that the excess power generated could present an opportunity for developing microgrids in neighboring villages with unreliable grid access. Additionally, the surplus electricity can be utilized for applications like water desalination or other deferrable loads. The results highlight the necessity of incorporating a bio-generator device to achieve economic efficiency while fulfilling environmental objectives. Technically, the presence of a generator enhances the flexibility of the power generation process and enables more cost-effective handling of load peaks. The optimality factor of the PV/WT/Bio/battery scenario exceeds 80% in both cases, indicating the consistent alignment of the results with sustainable development goals. The TOPSIS output, utilizing AHP and SDG weighting methods, demonstrates similar behavior in estimating optimal scenarios, with the SDG-based method yielding a higher optimality factor. Moreover, the SDG method exhibits a greater disparity between the best and worst scenarios, illustrating its superior performance compared to alternative methods.

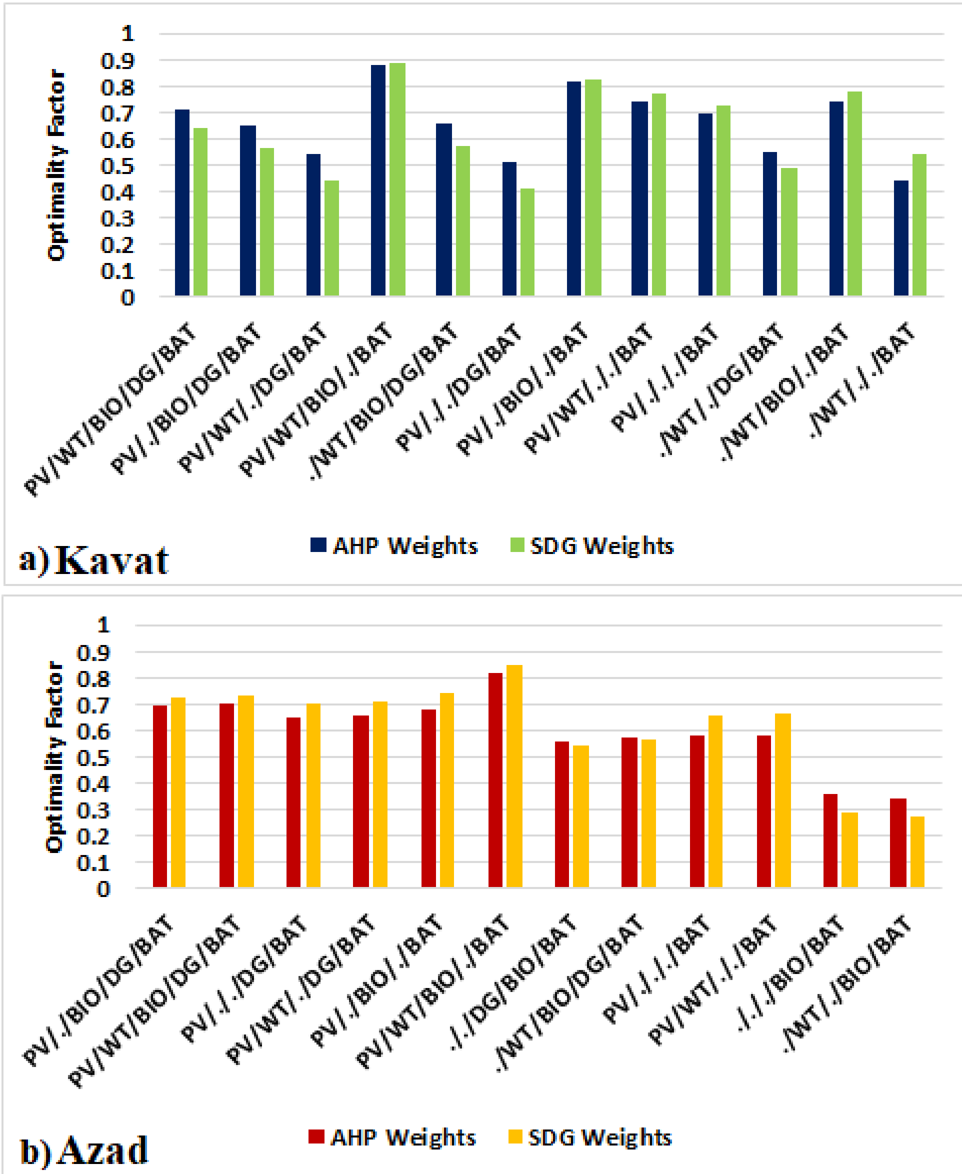

Fig. 8 TOPSIS method optimality factor for each optimum configuration of HOMER software.

6.3. Sensitivity/Uncertainty Analysis

In order to assess the economic stability of the optimal scenario obtained through the integrated HOMER-SDG-MCDM method, a sensitivity analysis is performed on the key input uncertainties. This analysis is conducted under the primary condition, considering an average of two case studies. The sensitivity analysis is shown in Fig. 9, indicating the capital cost of both WT and PV has a major effect on the COE. The cost multiplier changes from 0.7 to 1.3 (30% variation in the current capital) for both components leading to the COE in the range of 0.19 and 0.23 $/kWh, which implies a 9.2% decrease and 6.9% increase compared to the primary COE respectively. Furthermore, referring to the technical factor, the local resources chare decrease from more than 93% to about 85% when the renewable technology prices rise. The reasonable changes in renewables potential (solar radiation and wind speed) led to the COE range of about 0.17 and 0.23 $/kWh, while the highest slop of heat map color changes on PV resource potential demonstrates its higher effect on the economic affair of HRES.

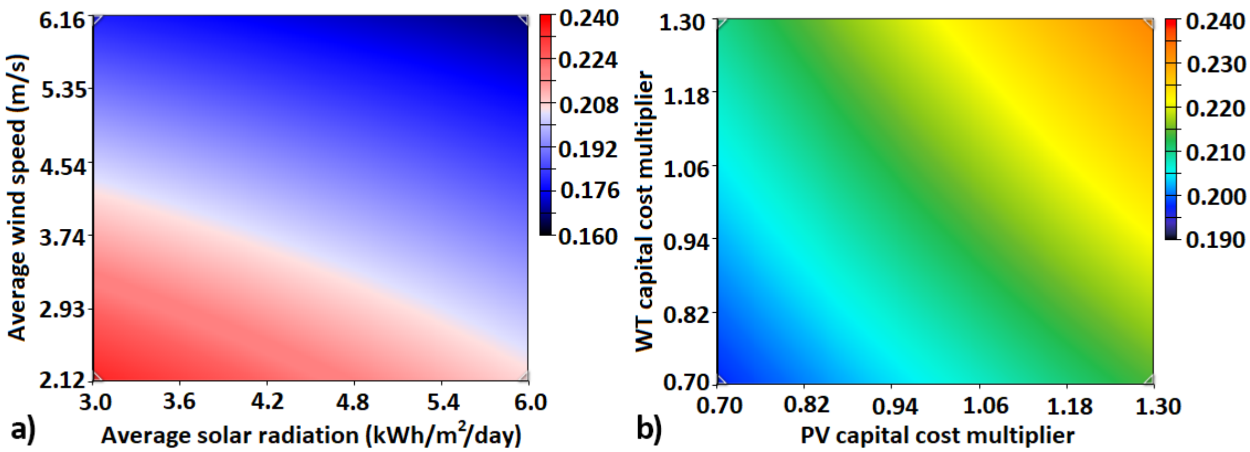

Fig. 9 Sensitivity of COE ($/kWh) to a) Uncertainty in renewable technology prices, and b) Uncertainty in available renewable potential

According to Fig. 10, changes in fuel prices have a more significant effect on COE compared to possible uncertainties in fuel generator capital costs. Considering prevalent diesel fuel changes in the western region of Asia, ranging from 0.2 to 0.5 $/L, and potential local biomass prices ranging from 5 to 15 $/ton (mainly due to waste collection fees), the COE will vary between 0.19 and 0.23 $/kWh. On the other hand, a possible 30% uncertainty in fuel generator capital costs results in COE changes of less than 0.02 $/kWh. Therefore, based on the outputs of Figs. 9 and 10, the sensitivity to possible local uncertainties is less than 0.05 $/kWh, demonstrating the economic stability of the optimal HRES introduced by the MCDM-SDG framework.

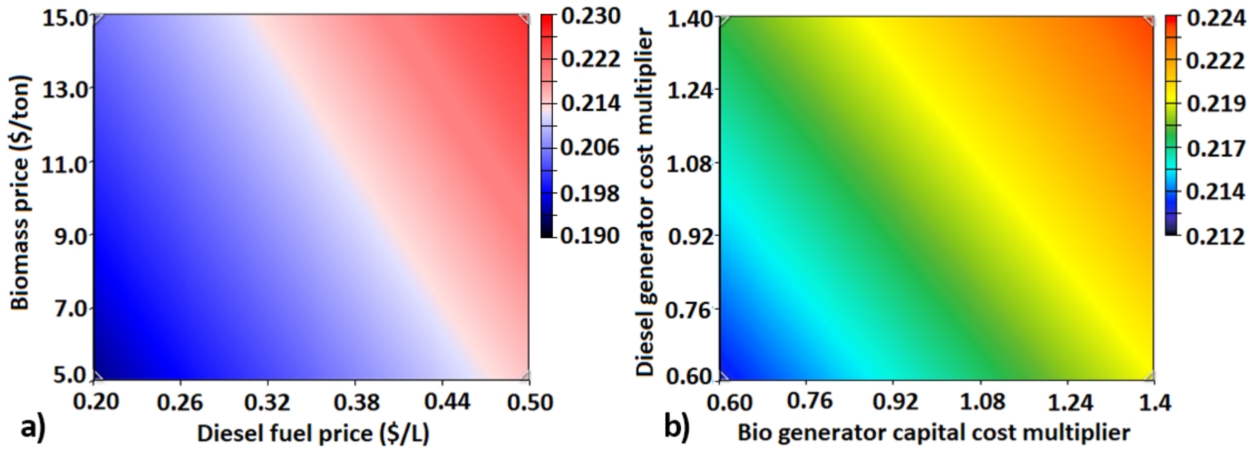

Fig. 10 Sensitivity of COE ($/kWh) to a) Uncertainty in fuel prices, and b) Uncertainty in generator capital cost

Based on Fig. 11, applying battery bank technologies with high throughput showed a slight improvement in energy cost, while the initial capital cost of the battery bank had a more significant effect on COE variation (approximately 0.03 $/kWh variation). In fact, the dependency of off-grid HRESs on the storage bank cost is evident in the sensitivity analysis of Li-ion batteries applied in the current study. Furthermore, according to this figure, improving demand and increasing power supply reliability (by reducing possible capacity shortages) showed the highest uncertainty, ranging from about 0.20 to 0.35 $/kWh. Although considering a maximum possible load increment of 10% and less than 2% capacity shortage, the COE will not exceed 0.25, which is acceptable for an off-grid application.

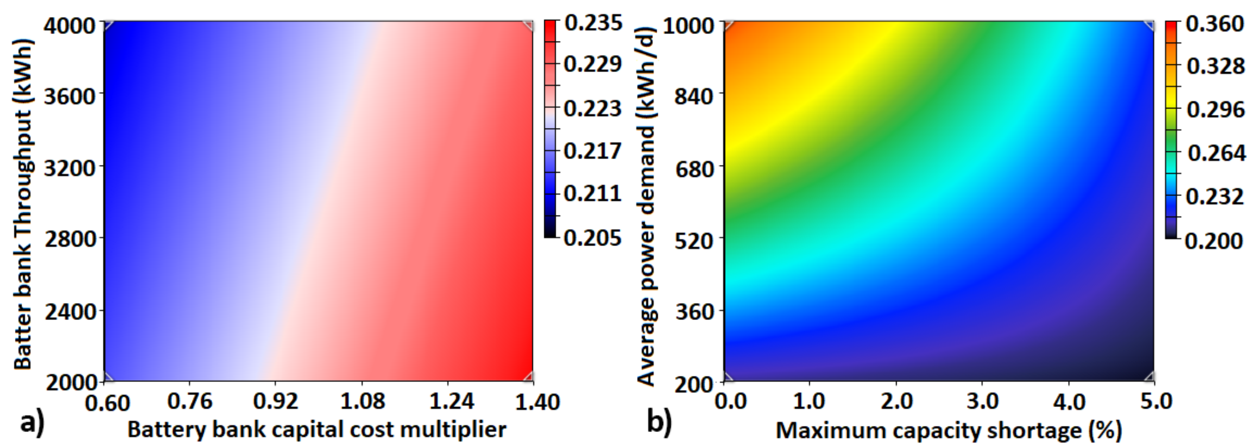

Fig. 11 Sensitivity of COE ($/kWh) to a) Uncertainty in fuel prices, and b) Uncertainty in generator capital cost

Figure 12(a) illustrates that when the capital cost of grid extension is less than 7,000 $/km, the distance to the nearest power grid must be more than 35 km for off-grid HRES to be affordable. Conversely, when this value exceeds 12,000 $/km, the grid breakeven distance can be within distances less than 20 km. This demonstrates the increased affordability of developed HRES in deprived areas located far from national transmission lines or in rugged terrains where the cost of developing power transmission lines is prohibitively high. Furthermore, Figure 12(b) demonstrates that as fuel availability decreases or becomes more uncertain, the COE tends to increase. Consequently, when the average diesel fuel availability is less than 10,000 L/yr, it becomes challenging to achieve an HRES with a cost lower than 0.24 $/kWh. Additionally, achieving an HRES with a cost below 0.23 $/kWh requires a biomass availability higher than 0.5 tons/day. Therefore, fuel availability plays a crucial role in maintaining the sustainability of the system.

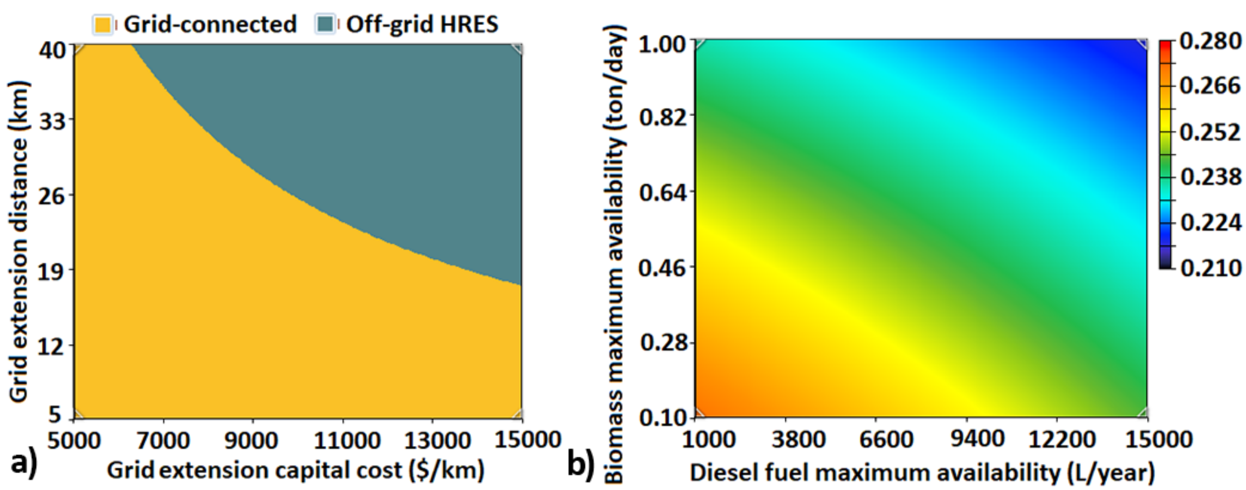

Fig. 12 a) Grid extension breakeven distance analysis, and b) COE sensitivity to uncertainty in fuel availability

6.4. Performance Comparison

The power generated by each component in the summer months is illustrated in Fig. 13 for two optimum scenarios using HOMER-MCDM and HOMER methods. As can be seen, in both scenarios, PV plays the main role in meeting the energy demand compared to other energy sources. The first scenario, consisting of PV/WT/bio/battery, is derived from the hybrid investigation of HOMER and MCDM. In this scenario, due to the absence of the diesel generator, higher renewable energy installations are implemented. The main difference between these two scenarios lies in the operation of fuel generators and batteries. With the diesel generator applied in the HRES, the fuel generator operates for a longer duration due to the low cost of diesel fuel. However, by employing the bio generator, the operation hours of the fuel generator decrease, allowing for higher capacities of wind turbine and battery bank installations. The bio generator only operates when the total generated renewable energy is lower than the demand in the optimum scenario of SDG-based MCDM. Conversely, in the absence of wind power generation, both diesel and bio generators must operate simultaneously in the optimum HOMER scenario. This approach, which offers greater energy generation flexibility through two generators, reduces the need for costly battery operation. However, this scenario results in higher CO_2 emissions and greater dependence on fuel, whereas the first scenario achieves an optimum system that relies 100% on renewable energy. Thus, SDG-MCDM prioritizes environmental objectives alongside economic considerations, while HOMER aims to select the most affordable system.

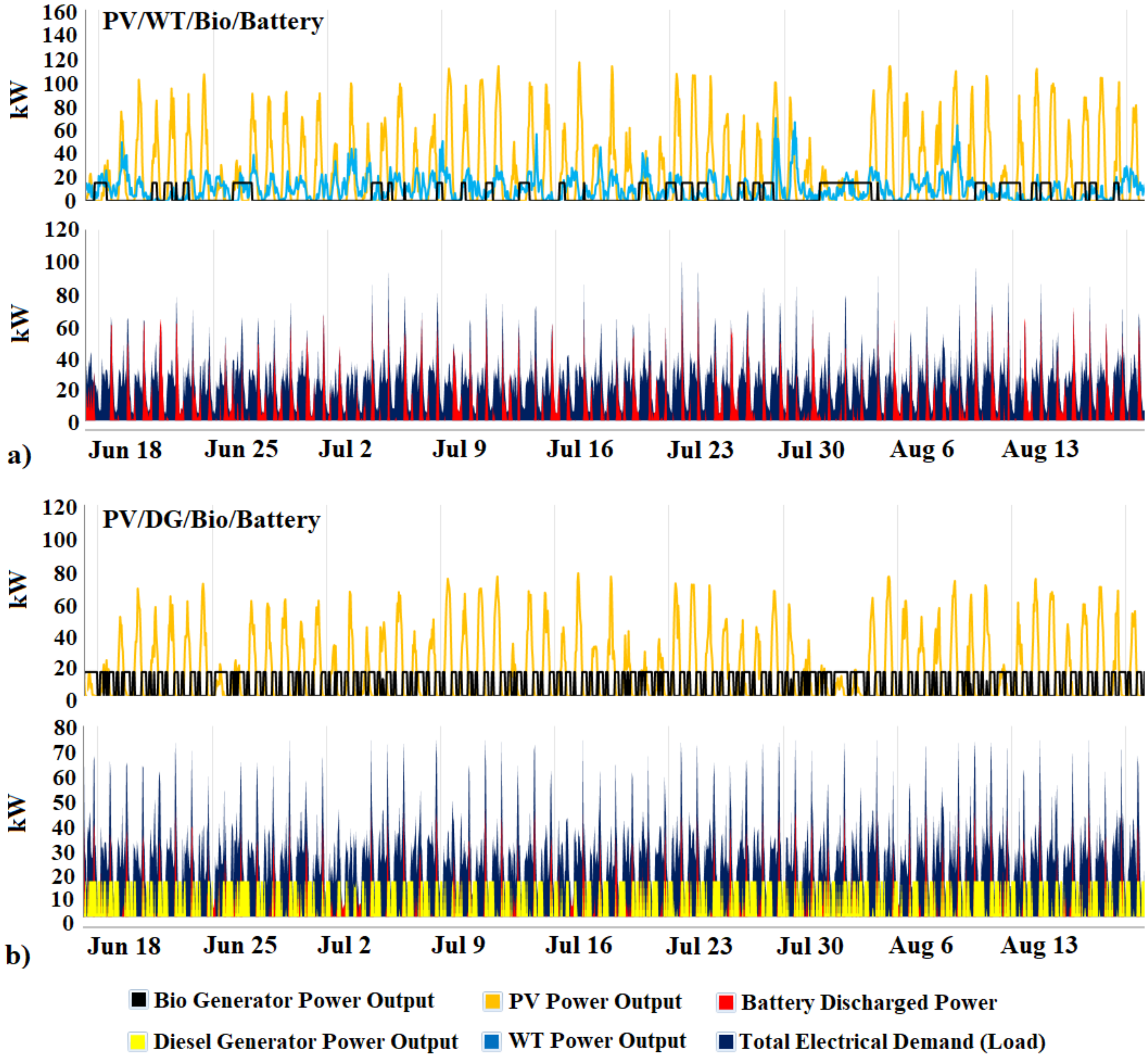

Fig. 13 The power supply process of hybrid renewable energy system during the summer: a) optimum scenario by the HOMER-MCDM method, and b) optimum scenario by the HOMER method

6.5. Policy discussion and comparative analysis

The international interest in SDG17 provides a common language and a shared vision for sustainable development, facilitating collaboration and knowledge sharing among different countries and regions. This is particularly relevant for rural areas HRESs can play a crucial role in providing access to clean and reliable energy, supporting economic development, and improving the quality of life for rural communities. The importance of rural development through renewable systems is emphasized by numerous studies every year, although the most economically viable power supply option for these areas may not always be the most environmentally friendly, energy-efficient, and reliable method. This poses an international challenge for decision-making.

The most widely available tools for investors and policymakers for developing renewable systems in different countries are commercial software programs, which primarily optimize energy solutions based on a single economic objective. However, numerous weighting approaches have been proposed today and combined with MCDM methods to overcome this limitation. Nonetheless, there is a significant need to implement a consistent global framework to mitigate the influence of subjective opinions on the weighting of energy system parameters, such as AHP-based methods, or in cases where reliable data is unavailable for policymakers to weigh the objectives by data-driven methods. Therefore, this study applies SDG17 of the United Nations to assign objective weights to the off-grid bio-based energy system for rural applications. SDG17 can also be relevant from governance, policy, and practical perspectives by providing a set of guidelines and indicators to monitor and evaluate the performance of HRESs. This can assist policymakers and practitioners in identifying areas for improvement, tracking progress toward sustainability goals, and making informed decisions regarding resource allocation and investment. Consequently, the utilization of SDG17 can serve as a valuable tool for promoting sustainable development in the context of hybrid energy system planning, particularly in rural areas.

This approach is also highly relevant to governance, particularly in the presence of national challenges for enhancing the quality of life in deprived and rural areas. SDG17 specifically focuses on partnerships for the goals, emphasizing the importance of collaboration and cooperation among different stakeholders, including governments, private sectors, and civil society, to achieve sustainable development. The significance of incorporating SDG17 into the planning of HRESs lies in its ability to provide a comprehensive framework for evaluating the sustainability of these systems. By considering economic, social, and environmental factors, SDG17 helps ensure that the planning and implementation of HRESs are not only economically viable but also socially inclusive and environmentally sustainable. Therefore, the proposed method in this study can be integrated with practical scenarios introduced by commercial energy optimization tools. This integration can assist policy makers in the development of renewable systems while considering all aspects of sustainable development.

The Power for All fact sheet, published in 2019 [83], stated that the average cost of a highly renewable stand-alone energy system is generally over 0.5 $/kWh. However, there is a need for methods to reduce this cost to less than 0.22 $/kWh by 2030 to achieve affordable power supply, which is one of the main objectives of the Sustainable Development Goals (SDGs). The sensitivity analysis of the HOMER-MCDM-SDG method demonstrated a range of COE from 0.18 to 0.24 $/kWh, while simultaneously addressing all aspects of sustainable development instead of solely relying on economic objectives. By referring to the optimum HRES energy cost of some recent studies applying bio-resources (Table 11), it is evident that off-grid cases demonstrate a range of COE from 0.17 to more than 0.43 $/kWh. This range affirms the appropriate cost of the proposed PV/WT/BG/Battery 100% renewable energy system. However, despite the positive findings, these studies also highlight major challenges in off-grid applications, including the management of excess electricity, ensuring system stability while relying on renewable resources, and minimizing unmet electrical load. Simultaneously addressing these aspects remains a significant challenge without applying reliable MCDM methods.

Table 11. Comparison of recent studies on utilizing bio-resources in hybrid renewable energy systems to provide economic profits

Study	System	Bio-resource	Load	COE (USD/kWh)	Main points
[84], 2023, Sierra Leone	PV/Bio-generator/Battery	Agricultural wastes	266 kWh/day	> 0.37	Due to the higher number of economic objectives, scenarios with greater economic viability have a

					higher chance of being optimal in different MCDM methods.
[85], 2023, Morocco	PV/Battery/Bio-walls	Plant fibers	11.2 kWh/day	> 0.21	The application of bio-based breaks resulted in more than 25% annual energy savings, providing a 100% renewable solution for rural areas.
[86], 2023, Brazil	PV/Bio-generator/Grid-sell back	Agricultural wastes	Large scale	< 0.10	The presence of a grid is essential to accommodate a high level of excess power injection and ensure affordability.
[87], 2022, Iran	PV/Bio-generator/Diesel-generator/Battery	Livestock residue	4219.4 kWh/day	> 0.17	Prioritizing economic objectives can lead to a reduction of more than 25% in the off-grid renewable fraction, particularly when the local fuel price is low.
[88], 2022, Qatar	PV/WT/Bio-generator/H_2&NH_3-generators/Battery	Waste oil and animal fat	1750 kWh/day	> 0.28	By employing different types of fuels in a countercurrent manner, the likelihood of achieving an affordable and reliable power supply with less than 1% unmet load is enhanced
[89], 2022, MENA	Grid-purchase/PV/Bio-generator/Diesel-generator/Battery	Plant waste, animal dung, and municipal solid waste	1098.3 kWh/day	> 0.43	When local fuel and grid tariffs are high, it becomes imperative to place more emphasis on renewable resources.
[90], 2021, India	PV/WT/Bio-generator/Diesel-generator/Battery	Organic wastes	Small scale	> 0.17	More than 90% of the power demand can be fulfilled by renewable resources, with the total fuel consumption level being a crucial factor affecting the COE.

Conclusion

The present study aims to examine a hybrid energy system designed to power two rural regions with different biomass sources including agricultural and animal-based resources. By conducting a sizing optimization process using HOMER software, it was revealed that the economically optimal scenario did not align with the desired outcomes for CO_2 emissions, energy efficiency, and reliability. This underscores the importance of employing multi-criteria decision-making for each specific case. In order to determine the most suitable renewable hybrid system, a comprehensive set of criteria including economic, environmental, technical, and energy security aspects were taken into account. Additionally, the Sustainable Development Goals were considered when assigning weights to these criteria, ensuring a holistic approach to the decision-making process.

Most conventional weighting methods for MCDM heavily rely on conventional AHP methods and expert opinions, often resulting in a higher prioritization of economic objectives for rural electrification. However, in this study, SDG-17, developed by the United Nations, is chosen as the primary criterion for determining the importance of decision parameters. Accordingly, each objective that aligns with a higher number of SDGs is assigned a higher weight. This approach, compared to conventional AHP-based methods, demonstrates higher weighted values for environmental and energy security factors, with increases of 14.2% and 10.7% respectively. Furthermore, the weighted values of the technical parameters remain relatively consistent, while the weights assigned to economic parameters are reduced to approximately 9.5%, compared to 12% in the AHP method. So, by considering the alignment of energy system parameters with the SDGs, decision-makers can take into account broader sustainability goals beyond just economic considerations.

The resulting optimum solution reduces CO_2 emissions by over 20% and displays significantly lower fuel dependency than HOMER's initial results. Moreover, sensitivity analyses were conducted on both the capital costs of power generation components and the potential of renewable resources. By adjusting the 30% possible variation in the investment costs of PV and WT units, the COE ranges from 0.198 to 0.233 $/kWh. Additionally, changes in biomass cost from 5 to 15 $/tonne and diesel pricing from 0.20 to 0.5 $/L can lead to COE variations in the range of 0.194 to

0.227 $/kWh, representing an approximate uncertainty of 9.2%. The optimum system with this method, with an energy cost of less than 0.22 $/kWh, a renewable fraction of more than 90%, and less than 27% excess electricity (resulting in more than 73% hybrid system energy efficiency), is attractive for rural electrification in deprived areas with potential bio-resources.

From a governance and policy maker's perspective, the optimal scenario, considering the SDG17 framework compared to a purely financial approach, leads to a more sustainable solution by reducing fossil fuel dependency, improving resource diversity, and decreasing CO_2 emissions. This sustainable solution maintains power supply reliability and achieves a cost below 0.25 $/kWh. However, despite a surplus of more than 10% electricity due to higher participation of renewables, further implementation of additional methods is necessary to improve the surplus power utilization index.

Although for Iranian deprived areas, the SDG-based and AHP-based MCDM showed almost similar optimum scenarios, it is suggested to analyze the proposed method in other regions of the world in future studies. This is because different situations may require different sets of criteria or weights, and it is essential to carefully evaluate and justify the selection of criteria, including the use of SDGs, based on the specific circumstances and stakeholders' priorities. Furthermore, it is suggested that other multi-criteria decision-making methods in modern integrated renewable systems with novel weighting methods will be investigated in the future.

Appendix A: MATLAB Codes for weighted TOPSIS method

```
Xval=length(X(:,1));
Y = zeros([Xval,length(W)]);
%% calculating the normalized matrix
for j=1:length(W)
   for i=1:Xval
   Y(i,j)=X(i,j)/sqrt(sum((X(:,j).^2)));
   end
end
Normalized_Matrix = num2str([Y])
%% calculating the weighted normalized matrix
for j=1:length(W)
   for i=1:Xval
      Yw(i,j)=Y(i,j).*W(j);
   end
end
Weighted_Normalized_Matrix = num2str([Yw])
%% calculating the positive and negative best
 for j=1:length(W)
   if Wcriteria(1,j)== 0
      Vp(1,j)= min(Yw(:,j));
      Vn(1,j)= max(Yw(:,j));
   else
      Vp(1,j)= max(Yw(:,j));
      Vn(1,j)= min(Yw(:,j));
   end
end
 Positive_best = num2str([Vp])
 Negative_best = num2str([Vn])
%% distance from Ideal Best and Worst
for j=1:length(W)
   for i=1:Xval
```

```
        Sp(i,j)=((Yw(i,j)-Vp(j)).^2);
        Sn(i,j)=((Yw(i,j)-Vn(j)).^2);
    end
end
for i=1:Xval
    Splus(i)=sqrt(sum(Sp(i,:)));
    Snegative(i)=sqrt(sum(Sn(i,:)));
end
%% calculating the performance score
P=zeros(Xval,1);
for i=1:Xval
    P(i)=Snegative(i)/(Splus(i)+Snegative(i));
end
Performance_Score =  num2str([P])
```

References

[1] García-Ferrero J, Merchán RP, Santos MJ, Medina A, Calvo Hernández A. Brayton technology for Concentrated Solar Power plants: Comparative analysis of central tower plants and parabolic dish farms. Energy Convers Manag 2022;271:116312. doi:https://doi.org/10.1016/j.enconman.2022.116312.

[2] Khirennas A, Talha A, Kaabeche A, Bakelli Y. Overview of fossil fuel-based hybrid power generation systems within mini-grids – The experience of storage-less PV system integration into three of the Great Algerian South mini-grids. Energy Convers Manag 2020;221:113191. doi:10.1016/j.enconman.2020.113191.

[3] Das BK, Alotaibi MA, Das P, Islam MS, Das SK, Hossain MA. Feasibility and techno-economic analysis of stand-alone and grid-connected PV/Wind/Diesel/Batt hybrid energy system: A case study. Energy Strateg Rev 2021;37:100673. doi:10.1016/j.esr.2021.100673.

[4] International Renewable Energy Agency (IRENA). World Energy Transitions Outlook 2022: 1.5°C Pathway, International Renewable Energy Agency, Abu Dhabi. 2022.

[5] Förster J, Vogt H. IEA (2020), World Energy Outlook 2020, IEA, Paris https://www.iea.org/reports/world-energy-outlook-2020 2010;109:47057.

[6] Rajaee F, Amin M, Rad V, Aliyon K, Kasaeian A. Techno-economic evaluation of an organic rankine cycle-based multi-source energy system for 100 % -renewable power supply : A rural case study. Sustain Cities Soc 2023;89:104290. doi:10.1016/j.scs.2022.104290.

[7] IEA (2020), Secure, Sustainable and Affordable Power Systems in Emerging Economies, IEA, Paris. https://www.iea.org/reports/secure-sustainable-and-affordable-power-systems-in-emerging-economies n.d.

[8] United Nations Department of Economic and Social Affairs. Transforming our world: the 2030 Agenda for Sustainable Development, 2015. http://www.un.org/ga/search/view_doc.asp?symbol=A/RES/70/1&Lang=E n.d.

[9] Niyommaneerat W, Suwanteep K, Chavalparit O. Sustainability indicators to achieve a circular economy: A case study of renewable energy and plastic waste recycling corporate social responsibility (CSR) projects in Thailand. J Clean Prod 2023;391:136203. doi:10.1016/j.jclepro.2023.136203.

[10] Paudel D, Jeuland M, Lohani SP. Cooking-energy transition in Nepal: Trend review. Clean Energy 2021;5:1–9. doi:10.1093/ce/zkaa022.

[11] Olabi AG, Abdelkareem MA, Al-Murisi M, Shehata N, Alami AH, Radwan A, et al. Recent progress in Green Ammonia: Production, applications, assessment; barriers, and its role in achieving the sustainable development goals. Energy Convers Manag 2023;277:116594. doi:10.1016/j.enconman.2022.116594.

[12] Pirmohamadi A, Dastjerdi SM, Ziapour BM, Ahmadi P, Rosen MA. Integrated solar thermal systems in smart optimized zero energy buildings: Energy, environment and economic assessments. Sustain Energy Technol Assessments 2021;48:101580. doi:10.1016/j.seta.2021.101580.

[13] Hossein Jahangir M, Bazdar E, Kargarzadeh A. Techno-economic and environmental assessment of low carbon hybrid renewable electric systems for urban energy planning: Tehran-Iran. City Environ Interact 2022;16:100085. doi:10.1016/j.cacint.2022.100085.

[14] Destek MA, Sarkodie SA, Asamoah EF. Does biomass energy drive environmental sustainability? An SDG perspective for top five biomass consuming countries. Biomass and Bioenergy 2021;149:106076. doi:10.1016/j.biombioe.2021.106076.

[15] Wang G, Liao Q, Zhang H, Liang Y. How government policies promote bioenergy's permeability in national-level energy supply chain: A case of China. Appl Energy 2022;324:119750. doi:10.1016/j.apenergy.2022.119750.

[16] World Bioenergy Association. Global Bioenergy Statistics 2020, https://www.worldbioenergy.org/uploads/201210 WBA GBS 2020.pdf. n.d.

[17] Razavi Dehkordi MH, Meghdadi Isfahani AH, Rasti E, Nosouhi R, Akbari M, Jahangiri M. Energy-Economic-Environmental assessment of solar-wind-biomass systems for finding the best areas in Iran: A case study using GIS maps. Sustain Energy Technol Assessments 2022;53:102652. doi:https://doi.org/10.1016/j.seta.2022.102652.

[18] Javed MS, Song A, Ma T. Techno-economic assessment of a stand-alone hybrid solar-wind-battery system for a remote island using genetic algorithm. Energy 2019;176:704–17. doi:10.1016/j.energy.2019.03.131.

[19] Paneri A, Moore K, Beylot A, Muller S, Braun M, Yan X. Renewable energy can make small-scale mining in Europe more feasible. Resour Conserv Recycl 2021;172:105674. doi:10.1016/j.resconrec.2021.105674.

[20] Huang Y, Wang Q, Xu J. A Stackelberg-based biomass power trading game framework in hybrid-wind/solar/biomass system: From technological, economic, environmental and social perspectives. J Clean Prod 2023;391:136203. doi:10.1016/j.jclepro.2023.136806.

[21] Yong CC, Rahman MM, Faizal HM, Saat A, Wahid MA. Techno-economic evaluation of hybrid power system in rural area of Sarawak, Malaysia. Proc Int Conf Ind Eng Oper Manag 2019:72–80.

[22] Middelhoff E, Andrade Furtado L, Peterseim JH, Madden B, Ximenes F, Florin N. Hybrid concentrated solar biomass (HCSB) plant for electricity generation in Australia: Design and evaluation of techno-economic and environmental performance. Energy Convers Manag 2021;240:114244. doi:10.1016/j.enconman.2021.114244.

[23] Singh S, Singh M, Kaushik SC. Feasibility study of an islanded microgrid in rural area consisting of PV, wind, biomass and battery energy storage system. Energy Convers Manag 2016. doi:10.1016/j.enconman.2016.09.046.

[24] Kharrich M, Kamel S, Alghamdi AS, Eid A, Mosaad MI, Akherraz M, et al. Optimal design of an isolated hybrid microgrid for enhanced deployment of renewable energy sources in Saudi Arabia. Sustain 2021;13:4708. doi:10.3390/su13094708.

[25] El-Sattar HA, Kamel S, Hassan MH, Jurado F. Optimal sizing of an off-grid hybrid photovoltaic/biomass gasifier/battery system using a quantum model of Runge Kutta algorithm. Energy Convers Manag 2022;258:115539. doi:https://doi.org/10.1016/j.enconman.2022.115539.

[26] Ahmad J, Imran M, Khalid A, Iqbal W, Ashraf SR, Adnan M, et al. Techno economic analysis of a wind-photovoltaic-biomass hybrid renewable energy system for rural electrification: A case study of Kallar Kahar. Energy 2018. doi:10.1016/j.energy.2018.01.133.

[27] Alshammari N, Asumadu J. Optimum unit sizing of hybrid renewable energy system utilizing harmony search, Jaya and particle swarm optimization algorithms. Sustain Cities Soc 2020;60:102255. doi:10.1016/j.scs.2020.102255.

[28] Jahangiri M, Rizi RA, Shamsabadi AA. Feasibility study on simultaneous generation of electricity and heat using renewable energies in Zarrin Shahr, Iran. Sustain Cities Soc 2018;38:647–61. doi:10.1016/j.scs.2018.01.043.

[29] Li J, Liu P, Li Z. Optimal design and techno-economic analysis of a solar-wind-biomass off-grid hybrid power system for remote rural electrification: A case study of west China. Energy 2020;208:118387. doi:10.1016/j.energy.2020.118387.

[30] Cano A, Arévalo P, Jurado F. Energy analysis and techno-economic assessment of a hybrid PV/HKT/BAT system using biomass gasifier: Cuenca-Ecuador case study. Energy 2020;202:117727. doi:10.1016/j.energy.2020.117727.

[31] Khan MU, Hassan M, Nawaz MH, Ali M, Wazir R. Techno-economic Analysis of PV/wind/biomass/biogas hybrid system for remote area electrification of Southern Punjab (Multan), Pakistan using HOMER Pro. 2018 Int. Conf. power Gener. Syst. Renew. energy Technol., IEEE; 2018, p. 1–6.

[32] Guo M, Liu G, Liao S. Normalized techno-economic index for renewable energy system assessment. Int J Electr Power Energy Syst 2021;133:107262. doi:10.1016/j.ijepes.2021.107262.

[33] Edrisi SA, Abhilash PC. Exploring marginal and degraded lands for biomass and bioenergy production: An Indian scenario. Renew Sustain Energy Rev 2016;54:1537–51. doi:10.1016/j.rser.2015.10.050.

[34] Das S, Pradhan S, De S. Multi criteria decision making for the most suitable combination of energy resources for a decentralized hybrid energy solution with green hydrogen as the storage option. Energy Convers Manag 2023;285:117028. doi:10.1016/j.enconman.2023.117028.

[35] Das S, De S. MCDM for simultaneous optimum economy , investment risk and environmental impact for distributed renewable power : Demonstration with an Indian village data. Energy Convers Manag 2023;277:116631. doi:10.1016/j.enconman.2022.116631.

[36] Song J, Liu C, Xing J, Yang W, Ren J. Linking bioenergy production by agricultural residues to sustainable development goals: Prospects by 2030 in China. Energy Convers Manag 2023;276:116568. doi:10.1016/j.enconman.2022.116568.

[37] Nandimandalam H, Aghalari A, Gude VG, Marufuzzaman M. Multi-objective optimization model for regional renewable biomass supported electricity generation in rural regions. Energy Convers Manag 2022. doi:10.1016/j.enconman.2022.115833.

[38] IEA (2020), Bioenergy Power Generation, IEA, Paris. https://www.iea.org/reports/bioenergy-power-generation n.d.

[39] Toopshekan A, Rahdan P, Vaziri Rad MA, Yousefi H, Astaraei FR. Evaluation of a stand-alone CHP-Hybrid system using a multi-criteria decision making due to the sustainable development goals. Sustain Cities Soc 2022;87:104170. doi:10.1016/j.scs.2022.104170.

[40] Javidmehr M, Pourfayaz F, Kasaeian A. Optimal design and analysis of a district energy system including heat and power production for domestic applications and fuel for vehicles. J Therm Anal Calorim 2021;144:2009–25. doi:10.1007/s10973-021-10631-7.

[41] Baneshi M, Hadianfard F. Techno-economic feasibility of hybrid diesel/PV/wind/battery electricity generation systems for non-residential large electricity consumers under southern Iran climate

conditions. Energy Convers Manag 2016;127:233–44. doi:10.1016/j.enconman.2016.09.008.

[42] Akhtari MR, Baneshi M. Techno-economic assessment and optimization of a hybrid renewable co-supply of electricity, heat and hydrogen system to enhance performance by recovering excess electricity for a large energy consumer. Energy Convers Manag 2019;188:131–41. doi:10.1016/j.enconman.2019.03.067.

[43] Roy D. Modelling an off-grid hybrid renewable energy system to deliver electricity to a remote Indian island. Energy Convers Manag 2023;281:116839. doi:10.1016/j.enconman.2023.116839.

[44] Khanalizadeh A, Razi F, Mahdi M. Experimental investigation of a PV / T system containing a TEG section between water-based heat exchanger and air-based heat sink. Therm Sci Eng Prog 2023;42:101909. doi:10.1016/j.tsep.2023.101909.

[45] Aier I, Anand A, Sakhiya AK, Kaushal P, Vijay VK. Modelling approaches to renewable energy sources for rural energy systems in India: a review and case study. Int J Ambient Energy 2022:1–14. doi:10.1080/01430750.2022.2085792.

[46] Manwell JF, McGowan JG. Lead acid battery storage model for hybrid energy systems. Sol Energy 1993;50:399–405. doi:10.1016/0038-092X(93)90060-2.

[47] Ribó-Pérez D, Herraiz-Cañete Á, Alfonso-Solar D, Vargas-Salgado C, Gómez-Navarro T. Modelling biomass gasifiers in hybrid renewable energy microgrids; a complete procedure for enabling gasifiers simulation in HOMER. Renew Energy 2021;174:501–12. doi:10.1016/j.renene.2021.04.083.

[48] Borum III L, McShane S, Richardson A. Mini-grids from Biomass Residue for Agricultural Circular Economy (MBRACE) 2021.

[49] Safieddin Ardebili SM. Green electricity generation potential from biogas produced by anaerobic digestion of farm animal waste and agriculture residues in Iran. Renew Energy 2020;154:29–37. doi:10.1016/j.renene.2020.02.102.

[50] Kasaeian A, Rahdan P, Rad MAV, Yan W-M. Optimal design and technical analysis of a grid-connected hybrid photovoltaic/diesel/biogas under different economic conditions: A case study. Energy Convers Manag 2019;198:111810. doi:10.1016/j.enconman.2019.111810.

[51] Heydari A, Askarzadeh A. Optimization of a biomass-based photovoltaic power plant for an off-grid application subject to loss of power supply probability concept. Appl Energy 2016;165:601–11. doi:10.1016/j.apenergy.2015.12.095.

[52] Güğül GN. Optimum hybrid renewable energy system design for on and off grid buildings: Hotel, education and animal hospital building case. Sol Energy 2023;253:414–27. doi:10.1016/j.solener.2022.12.044.

[53] Vaziri Rad MA, Panahi Vaghar M, Kouravand A, Bellos E, Kasaeian A. Techno-economic evaluation of stand-alone energy supply to a health clinic considering pandemic diseases (COVID-19) challenge. Sustain Energy Technol Assessments 2022;51:101909. doi:10.1016/j.seta.2021.101909.

[54] Parvin M, Yousefi H, Noorollahi Y. Techno-economic optimization of a renewable micro grid using multi-objective particle swarm optimization algorithm. Energy Convers Manag 2023;277:116639. doi:10.1016/j.enconman.2022.116639.

[55] Ghodusinejad MH, Lavasani Z, Yousefi H. A combined decision-making framework for techno-enviro-economic assessment of a commercial CCHP system. Energy 2023;276:127609. doi:10.1016/j.energy.2023.127609.

[56] Das S, Pradhan S, De S. Multi criteria decision making for the most suitable combination of energy resources for a decentralized hybrid energy solution with green hydrogen as the storage option. Energy Convers Manag 2023;285:117028. doi:10.1016/j.enconman.2023.117028.

[57] Shah KK, Mundada AS, Pearce JM. Performance of U.S. hybrid distributed energy systems: Solar photovoltaic, battery and combined heat and power. Energy Convers Manag 2015. doi:10.1016/j.enconman.2015.07.048.

[58] Statistical Center of Iran , Plan and Budget Organization, Presidency of the I.R.I., https://www.amar.org.ir/english n.d.

[59] https://earth.google.com/web. n.d.

[60] Amin M, Rad V, Kasaeian A, Niu X, Zhang K, Mahian O. Excess electricity problem in off-grid hybrid renewable energy systems : A comprehensive review from challenges to prevalent solutions.

Renew Energy 2023;212:538–60. doi:10.1016/j.renene.2023.05.073.

[61] Shahsavari A, Amin M, Rad V, Pourfayaz F, Kasaeian A. Optimal sizing of an integrated CHP and desalination system as a polygeneration plant for supplying rural demands. Energy 2022;258:124820. doi:10.1016/j.energy.2022.124820.

[62] Maleki A, Pourfayaz F, Ahmadi MH. Design of a cost-effective wind/photovoltaic/hydrogen energy system for supplying a desalination unit by a heuristic approach. Sol Energy 2016;139:666–75. doi:10.1016/j.solener.2016.09.028.

[63] Meteonorm Version 8, https://meteonorm.com/en/meteonorm-version-8. n.d.

[64] Maghanaki MM, Ghobadian B, Najafi G, Galogah RJ. Potential of biogas production in Iran. Renew Sustain Energy Rev 2013;28:702–14. doi:10.1016/j.rser.2013.08.021.

[65] Das BK, Hoque N, Mandal S, Pal TK, Raihan MA. A techno-economic feasibility of a stand-alone hybrid power generation for remote area application in Bangladesh. Energy 2017;134:775–88. doi:https://doi.org/10.1016/j.energy.2017.06.024.

[66] Mousavi SA, Toopshekan A, Mehrpooya M, Delpisheh M. Comprehensive exergetic performance assessment and techno-financial optimization of off-grid hybrid renewable configurations with various dispatch strategies and solar tracking systems. Renew Energy 2023;210:40–63. doi:10.1016/j.renene.2023.04.018.

[67] Taghizadeh-Alisaraei A, Hosseini SH, Ghobadian B, Motevali A. Biofuel production from citrus wastes: A feasibility study in Iran. Renew Sustain Energy Rev 2017;69:1100–12. doi:10.1016/j.rser.2016.09.102.

[68] Karimi Alavijeh M, Yaghmaei S. Biochemical production of bioenergy from agricultural crops and residue in Iran. Waste Manag 2016;52:375–94. doi:10.1016/j.wasman.2016.03.025.

[69] Safieddin Ardebili SM, Khademalrasoul A. An analysis of liquid-biofuel production potential from agricultural residues and animal fat (case study: Khuzestan Province). J Clean Prod 2018;204:819–31. doi:10.1016/j.jclepro.2018.09.031.

[70] Wang X, Mendelsohn R. An economic analysis of using crop residues for energy in China. Environ Dev Econ 2003;8:467–80. doi:10.1017/s1355770x0300251.

[71] Khan EU, Martin AR. Optimization of hybrid renewable energy polygeneration system with membrane distillation for rural households in Bangladesh. Energy 2015. doi:10.1016/j.energy.2015.09.109.

[72] Upadhyay DS, Sakhiya AK, Panchal K, Patel AH, Patel RN. Effect of equivalence ratio on the performance of the downdraft gasifier – An experimental and modelling approach. Energy 2019;168:833–46. doi:10.1016/j.energy.2018.11.133.

[73] Vaghefi SA, Keykhai M, Jahanbakhshi F, Sheikholeslami J, Ahmadi A, Yang H, et al. The future of extreme climate in Iran. Sci Rep 2019;9:1464. doi:10.1038/s41598-018-38071-8.

[74] Mousavi SA, Mehrpooya M, Rad MAV, Jahangir MH. A new decision-making process by integration of exergy analysis and techno-economic optimization tool for the evaluation of hybrid renewable systems. Sustain Energy Technol Assessments 2021;45:101196. doi:10.1016/j.seta.2021.101196.

[75] Emad D, El-Hameed MA, Yousef MT, El-Fergany AA. Computational Methods for Optimal Planning of Hybrid Renewable Microgrids: A Comprehensive Review and Challenges. Arch Comput Methods Eng 2020;27:1297–319. doi:10.1007/s11831-019-09353-9.

[76] Sinha S, Chandel SS. Review of software tools for hybrid renewable energy systems. Renew Sustain Energy Rev 2014;32:192–205. doi:10.1016/j.rser.2014.01.035.

[77] Fodhil F, Hamidat A, Nadjemi O. Potential, optimization and sensitivity analysis of photovoltaic-diesel-battery hybrid energy system for rural electrification in Algeria. Energy 2019;169:613–24. doi:10.1016/j.energy.2018.12.049.

[78] Yu G, Meng Z, Ma H, Liu L. An adaptive Marine Predators Algorithm for optimizing a hybrid PV/DG/Battery System for a remote area in China. Energy Reports 2021;7:398–412. doi:10.1016/j.egyr.2021.01.005.

[79] Singh S, Singh M, Kaushik SC. Feasibility study of an islanded microgrid in rural area consisting of PV, wind, biomass and battery energy storage system. Energy Convers Manag 2016;128:178–90. doi:10.1016/j.enconman.2016.09.046.

[80] Yazdani H, Baneshi M, Yaghoubi M. Techno-economic and environmental design of hybrid energy

systems using multi-objective optimization and multi-criteria decision making methods. Energy Convers Manag 2023;282:116873. doi:10.1016/j.enconman.2023.116873.

[81] Sedghiyan D, Ashouri A, Maftouni N, Xiong Q, Rezaee E, Sadeghi S. Prioritization of renewable energy resources in five climate zones in Iran using AHP, hybrid AHP-TOPSIS and AHP-SAW methods. Sustain Energy Technol Assessments 2021;44. doi:10.1016/j.seta.2021.101045.

[82] Rad MAV, Shahsavari A, Rajaee F, Kasaeian A, Pourfayaz F, Yan W-M. Techno-economic assessment of a hybrid system for energy supply in the affected areas by natural disasters: a case study. Energy Convers Manag 2020;221:113170.

[83] Power for All. Power for All Fact Sheet Potential O&M Cost Saving From Remote Monitoring. 2019.

[84] Konneh KV, Adewuyi OB, Gamil MM, Fazli AM, Senjyu T. A scenario-based multi-attribute decision making approach for optimal design of a hybrid off-grid system. Energy 2023;265:125663. doi:10.1016/j.energy.2022.125663.

[85] El Hassani S, Charai M, Moussaoui MA, Mezrhab A. Towards rural net-zero energy buildings through integration of photovoltaic systems within bio-based earth houses: Case study in Eastern Morocco. Sol Energy 2023;259:15–29. doi:10.1016/j.solener.2023.05.007.

[86] de Sá Machado VA, de Souza CG, Gonçalves MMBP, Chaves CF, Boloy RAM. Techno-economic feasibility analysis of biogas-solar photovoltaic hybrid system for bioenergy generation: a case study in the municipality of Boa Esperança (Pará, Brazil). Biomass Convers Biorefinery 2023. doi:10.1007/s13399-023-03978-4.

[87] Jahangir MH, Montazeri M, Mousavi SA, Kargarzadeh A. Reducing carbon emissions of industrial large livestock farms using hybrid renewable energy systems. Renew Energy 2022;189:52–65. doi:10.1016/j.renene.2022.02.022.

[88] Al Wahedi A, Bicer Y. Techno-economic optimization of novel stand-alone renewables-based electric vehicle charging stations in Qatar. Energy 2022;243:123008. doi:10.1016/j.energy.2021.123008.

[89] Al-Najjar H, El-Khozondar HJ, Pfeifer C, Al Afif R. Hybrid grid-tie electrification analysis of bio-

shared renewable energy systems for domestic application. Sustain Cities Soc 2022;77:103538. doi:10.1016/j.scs.2021.103538.

[90] Suman GK, Guerrero JM, Roy OP. Optimisation of solar/wind/bio-generator/diesel/battery based microgrids for rural areas: A PSO-GWO approach. Sustain Cities Soc 2021;67:102723. doi:10.1016/j.scs.2021.102723.